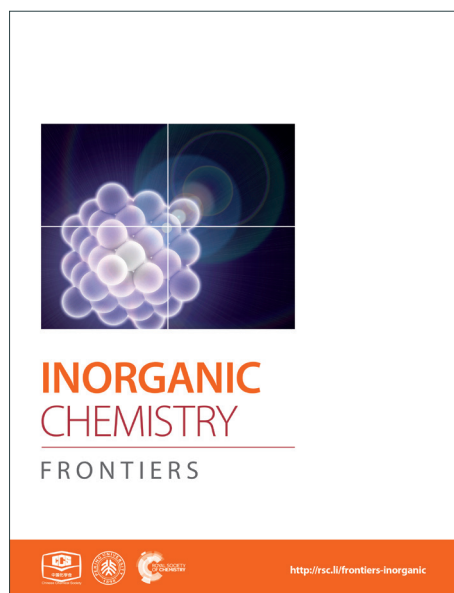
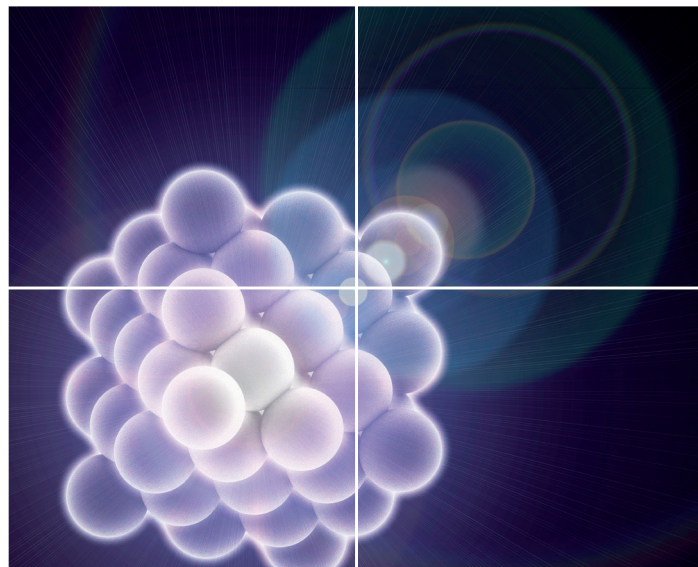


# INORGANIC CHEMISTRY

FRONTIERS

Accepted Manuscript



This is an *Accepted Manuscript*, which has been through the Royal Society of Chemistry peer review process and has been accepted for publication.

*Accepted Manuscripts* are published online shortly after acceptance, before technical editing, formatting and proof reading. Using this free service, authors can make their results available to the community, in citable form, before we publish the edited article. We will replace this *Accepted Manuscript* with the edited and formatted *Advance Article* as soon as it is available.

You can find more information about *Accepted Manuscripts* in the [Information for Authors](#).

Please note that technical editing may introduce minor changes to the text and/or graphics, which may alter content. The journal's standard [Terms & Conditions](#) and the [Ethical guidelines](#) still apply. In no event shall the Royal Society of Chemistry be held responsible for any errors or omissions in this *Accepted Manuscript* or any consequences arising from the use of any information it contains.

## CRITICAL REVIEW

# Metal phosphonate hybrid materials: from densely layered to hierarchically nanoporous structures

Cite this: DOI: 10.1039/x0xx00000x

Yun-Pei Zhu,<sup>a</sup> Tian-Yi Ma,<sup>a</sup> Ya-Lu Liu,<sup>a</sup> Tie-Zhen Ren<sup>b</sup> and Zhong-Yong Yuan\*<sup>a</sup>Received 00th January 2012,  
Accepted 00th January 2012

DOI: 10.1039/x0xx00000x

[www.rsc.org/](http://www.rsc.org/)

Metal phosphonate materials represent a promising member of non-siliceous inorganic-organic hybrids that are synthesized by combining metal joints and organophosphonic linkages at the molecular scale. The mild conditions for metal phosphonate synthesis, the homogeneous composition and the combined merits of inorganic units and organic groups have permitted the rational design and the incorporation of various functionalities through constituent building units. In this *critical review*, we present the development and recent advances related to the field of metal phosphonates and the relevant nanocomposites. Possibility to integrate the functionalities from both inorganic and organic moieties is discussed. Incorporation of well-defined porosity and capacity to be post-modified have extended the application potential to the area of adsorption, separation, catalysis, environmental remediation, energy storage and biology. Metal phosphonates thus present an unprecedented opportunity for the rational and precise design of sophisticated materials with multifunctionality.

## 1 Introduction

Deliberate effort to combine the superiorities of the inorganic units and organic moieties in a single composite material is an old challenge starting with the beginning of the industrial era. With “*chimie douce*”, Livage opened the gate towards a new galaxy of materials, inorganic-organic hybrid materials.<sup>1-5</sup> Noticeably, the concept of “inorganic-organic hybrid materials” has more to do with chemistry than with simple physical mixtures. In general, inorganic-organic hybrid materials are considered as nanocomposites with the inorganic and organic components interacted intimately at a molecular scale.<sup>6-10</sup>

Nowadays the field of organic-inorganic materials has been extended to other fields as diverse as molecular and supramolecular materials or polymer chemistry.<sup>11,12</sup> Furthermore, due to the combined physicochemical merits of organic and inorganic components, a very significant trend has been the growing research interest towards functional hybrids, which extends the field even broader and further. In addition to structural hybrid materials, there is a quickly expanding area of research on functional materials that focus on chemical, electrochemical, and biochemical activities, as well as on magnetic, electronic, and optical properties, or a combination of them.<sup>13</sup> The particular nanostructures, the degree of organization and the properties for the hybrid materials certainly depend on the chemical nature of the building

components, but they are also affected by the interactions among these components.

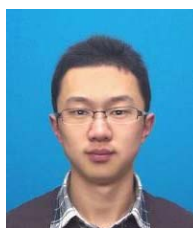
The key point for designing new hybrids is to adjust the nature, the extent and accessibility of the inner interfaces. As a result, the nature of the interface and the interactions exchanged by the organic and inorganic units can be employed to categorize the hybrids into two main classes.<sup>14-16</sup> Class I corresponds to the hybrid systems that involve no covalent or weak chemical bonding. In this class, only hydrogen bonding, Van der Waals or electrostatic forces are usually present. Reversely, Class II hybrid materials are those that show strong chemical interactions between the components, which are formed when the discrete inorganic building blocks are covalently bonded to the organic polymer or inorganic and organic polymers are covalently connected with each other.<sup>17,18</sup> On the other hand, hybrids can also be characterized by the type and size of the organic or the inorganic precursors.<sup>14,15</sup> Precursors can be two separate monomers or polymers and even covalently linked ones. Because of mutual insolubility between inorganic and organic components, phase separation will occur. However, homogeneous or single-phased hybrids can be obtained through judiciously choosing bifunctional monomers that contain organic and inorganic components, or by combining both types of components in phases where one of them is in large excess.<sup>19</sup>

The chemical strategies to construct Class II hybrid frameworks rely on the relative stability of the interactions between the components and the chemical linkages that

associate different components. Periodic mesoporous organosilicas (PMOs) containing organic siloxane groups in the silica network have received much attraction since 1999.<sup>20-22</sup> The stable Si-C bonds under hydrolytic conditions make it easily incorporate a large variety of organic bridges in the silica network during the sol-gel process. Nevertheless, besides the limited choice and high cost of the precursors of organosilicane, functionalization or modification of organosilicas is confined to the physical properties concerned with adsorption, ion-exchange and catalysis, and thereby the rational design of hybrid materials has been extended to non-siliceous organic-inorganic hybrid materials including metal sulfonates, carboxylates and phosphonates.<sup>23</sup> In comparison with the sulfonate and carboxylate counterparts, metal phosphonates exhibit much higher thermal and chemical stability due to the strong affinity of organophosphonic linkers to metal ions, making them promising in the fields of energy conversion, adsorption/separation, catalysis, biotechnology and so forth.<sup>23-25</sup> Furthermore, various organophosphonic acids and corresponding derivatives (*i.e.*, salts and esters) have been discovered in nature. Judicious design of the phosphonic bridging groups can introduce fantastic properties into the hybrid frameworks. The different reactivity of phosphonic coupling molecules leads to structural diversity and physicochemical peculiarities of the resultant hybrid materials and may provide decisive advantages in the sol-gel synthesis of

homogeneous hybrids. Chemical and thermal stability of phosphorus-carbon bonds in phosphonates may be considerably high against the hydrolysis. By using organically bridged phosphonic acids as coupling molecules, the homogeneous and efficient incorporation of organic functional groups into the framework of the materials can be realized, allowing the uniform physicochemical properties from the external surface to the internal skeleton.

Porosity endows materials with higher surface area, larger pore volume and lower density as compared with dense materials, thus allowing atoms, ions, molecules and even large guest molecules interact with the host materials not only at the surface but also throughout the bulk.<sup>26,27</sup> According to the IPUAC convention,<sup>28</sup> the porous materials are divided into three types depending upon the pore size: microporous, mesoporous, and macroporous materials with pores smaller than 2 nm, ranging from 2 to 50 nm, and larger than 50 nm, respectively. The distribution of shapes and sizes of the void spaces in nanoporous material is intimately related to their capability to perform desired function in a particular area. The demand to create uniformity in pore sizes and shapes and considerable volumes has been steadily increased over the past decades, which can lead to superior physicochemical properties. For instance, zeolites with uniform micropores can be employed to separate molecules on the basis of the pore size by selectively adsorb smaller molecules from a mixture containing molecules too large to enter into the pores. Noticeably,



Yun-Pei Zhu

*Yun-Pei Zhu received his BSc degree in 2011 at Henan Polytechnic University. He is currently a PhD candidate under the supervision of Prof. Zhong-Yong Yuan at Nankai University. His current research relates to the rational design and practical applications of porous inorganic-organic hybrid materials.*



Tian-Yi Ma

*Tian-Yi Ma received his BSc and PhD degrees in Chemistry at Nankai University in 2008 and 2013, respectively, under the supervision of Prof. Zhong-Yong Yuan. He is currently a postdoctoral research fellow in School of Chemical Engineering, the University of Adelaide, Australia.*



Ya-Lu Liu

*Ya-Lu Liu received her BSc degree in 2012 at Langfang Teachers University. She is currently a graduate student under the supervision of Prof. Zhong-Yong Yuan. Her current research is focused on the synthesis and application exploration of inorganic-organic hybrid materials.*



Tie-Zhen Ren

*Tie-Zhen Ren obtained her PhD degree from the University of Namur, Belgium in 2005. After two-year postdoctoral research at Stockholm University, Sweden, she joined the faculty of the Hebei University of Technology in 2007, where she is currently Professor in Chemical Technology. Her group's research areas include nanoporous photoelectrochemical materials and metal-organic frameworks.*



Zhong-Yong Yuan

*Zhong-Yong Yuan received his PhD degree from Nankai University in 1999. After his postdoctoral research at the Institute of Physics, Chinese Academy of Sciences, he joined the Laboratory of Inorganic Materials Chemistry at the University of Namur, Belgium in 2001. In 2005, he was engaged as a Professor in Nankai University. In 2006, he was awarded the "Program for New Century Excellent Talents in University" by the Ministry of Education. His research interests are mainly focused on the self-assembly of hierarchically nanoporous and nanostructured materials for energy and environmental applications.*

incorporation of well-structured porosity into the metal phosphonate frameworks can enhance the accessibility to the interior pore system. Therefore, functions due to inorganic units and organic moieties and their combined properties are valuable and interesting for the further exploration of porous metal phosphonate hybrid materials.

Recently, Kimura reviewed briefly the development of mesoporous aluminium organophosphonates prepared by the surfactant-assisted reactions between metal sources and bisphosphonates.<sup>29</sup> Clearfield *et al.* summarized the porous pillared zirconium and tin(IV) diphosphonates.<sup>30</sup> Indeed, mesoporous non-siliceous hybrids including metal sulfonates, carboxylates and phosphonates have been considered as a promising platform for designing multifunctional materials.<sup>23</sup> The synthesis of mesostructured titanium phosphonate hybrids has attracted tremendous interest due to the extended functions for clean energy and other applications.<sup>31</sup> Complicated porosity (from microporosity to macroporosity and even porous hierarchy) and various composition of hybrid framework (inorganic metal centers and organophosphonic linkage) can lead to remarkable physicochemical properties. The present *critical review* provides the comprehensive understanding of metal phosphonate hybrids from densely layered to porous networks, as well as the surface-phosphonated oxides. The key elements in rational design and synthesis of phosphonate-based hybrids are discussed. Moreover, the typical and emerging applications in the fields ranging from conventional catalysis and adsorption to the burgeoning biotechnology and energy conversion and storage are elaborated, in an attempt to attract more exploration interest in these innovative hybrid materials.

## 2 Crystalline metal phosphonates

Crystalline metal phosphonate hybrids, usually known as phosphonate-based metal-organic frameworks (MOFs), represent a particularly versatile field. Nonetheless, the phosphonate-based MOFs are considerably rarer than the carboxylate-based counterparts. This is mainly due to the less predictable coordination chemistry of phosphonate linkers and the more possible ligating modes,<sup>32</sup> leading to form densely layered structures that are poorly porous. This has prohibited the applications as adsorbents. Thus various tactics have been carried out to create porosity in metal phosphonates, such as utilizing multidimensional polyphosphonate ligands with spatially divergent phosphonate groups to generate open frameworks. In this section, the development of the crystalline metal phosphonate materials from layered structures to microporous or open-framework structure is exhibited.

### 2.1 Dense layered metal phosphonate materials

Metal phosphates have been studied as layered inorganic networks, which can be evolved into the field of inorganic-organic hybrids by appending the organic pillars off the rigid inorganic layers.<sup>13,33,34</sup> Layered structures are predominant for most metals with the organic groups being oriented perpendicularly into the interlamellar region (Fig. 1).<sup>35,36</sup> Thus

the interlayer distance can be easily tuned by changing the pillar groups and it is even possible to exfoliate the layers into film.<sup>37</sup> Pendant groups can impart other functionalities including chirality<sup>38</sup> and photoactivity.<sup>39</sup> Some initial layered metal phosphonate materials with very simple structures emerged decades ago. Alberti *et al.* reported the first layered zirconium phenylphosphonate and alkylphosphonates.<sup>40</sup> The structure of the phenylphosphonate was solved from the powder XRD patterns, yielded only 35-40 reflections that even after a long reflux time in HF acid rather than the hundred or more expected for a complex structure. Zirconium alkylphosphonates have structures similar to that of the phenylphosphonate, that is to say, they possessed  $\alpha$ -type layers. Layered metal phosphonates with monophosphonates are polymeric species that contain alternating hydrophilic and hydrophobic regions. In these compounds, the oxygen-bridged metal atoms form the central two-dimensional layers that are separated on either side by the pendant organic moieties of the phosphonate group. Many derivatives based on these initial works were also reported later. For example, zirconium phenylphosphonate could be sulfonated by treatment with fuming sulfuric acid to generate metal sulfophosphonates,<sup>41</sup> demonstrating the great potential in solid-acid catalysis and proton conductivity. It was found that layered polyether phosphates and phosphonates of zirconium could swell in water and complete exfoliation occurred when the value of  $n$  for the polyether chain,  $(\text{CH}_2\text{CH}_2\text{O})_n$ , was greater than nine.

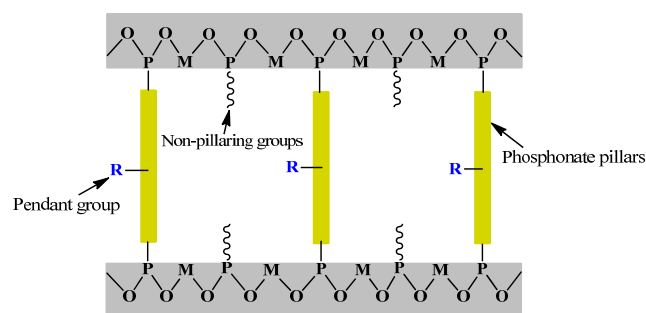


**Fig. 1** Schematic representation of layered metal phosphonates. To improve the porosity, one way is to insert small non-pillaring "spacer" groups, including metal oxide clusters, phosphoric, phosphoric, methylphosphonic acids, and crown ethers, between the phosphonate pillars. Another route is to attach pendant functional groups, such as imino, pyridine, hydroxyl, carboxylic and sulfonic acid, on the organophosphonic linkages.

Noticeably, because of their low solubility, metal phosphonates tend to be less crystalline than carboxylates. Also, phosphonate ligands do not form the types of secondary building units with metal ion joints as the carboxylates do, so the rational design of desired structures is considerably difficult. Toxic hydrofluoric acid is usually used to enhance the crystallization of the resultant frameworks.<sup>42-44</sup> Alternatively, additional function groups such as crown ether, carboxylate, hydroxyl, and amine groups have been attached to the phosphonic acid ligand to improve the solubility and crystallinity of phosphonates.<sup>45</sup> Several lanthanide phosphonates with a crown ether or calixarene moiety have

been reported.<sup>46-49</sup> A series of *N*-(phosphonomethyl) aza-crown ethers were prepared and reacted with M(IV) and M(II) ions.<sup>48</sup> With respect to zirconium phosphonates, the layered compounds have structures similar to those of the *N*-(phosphonomethyl)iminodiacetic acid. These compounds have been described as macroscopic leaflets since the crown ether portions resemble leaves bound to twigs. The interlayer spacing is 20 Å, indicating that there is no interdigitation of crown ether groups. Sulfonate groups were also incorporated into the metal phosphonate frameworks. Mao *et al.* synthesized a series of novel layered lanthanide sulfonate-phosphonates through hydrothermal reactions of lanthanide metal salts with MeN(CH<sub>2</sub>CO<sub>2</sub>H)(CH<sub>2</sub>PO<sub>3</sub>H<sub>2</sub>) and 5-sulfoisophthalic acid monosodium salt (NaH<sub>2</sub>BTS).<sup>49</sup> This reveals that by using a second metal linker such as carboxylic or sulfonic acids whose lanthanide complexes have better solubility in water and other solvent, the solubility and crystallinity of lanthanide phosphonates can thereby be greatly improved, which allows us to determinate their structures accurately and easily.

The elucidation of the structures of lanthanide phosphonates is quite significant and valuable due to the meaningful luminescent properties. Rare-earth elements as the metallic nodes in the construction of multidimensional phosphonate-based coordination polymers have been widely investigated, with the ultima objective of isolating novel photoluminescent materials.<sup>50,51</sup> The use of the polyfunctional tetraphosphonic acid ligand, (H<sub>2</sub>O<sub>3</sub>PCH<sub>2</sub>)<sub>2</sub>NCH<sub>2</sub>CH<sub>2</sub>CH<sub>2</sub>CH<sub>2</sub>N(CH<sub>2</sub>PO<sub>3</sub>H<sub>2</sub>)<sub>2</sub>, in combination with oxalic acid, gave rise to two different types of lanthanide-based luminescent frameworks.<sup>52</sup> Moreover, magnetism has been another focus for metal phosphonates, of which cobalt phosphonates prove to be the typical examples. In the framework of a layered cobalt carboxylate-phosphonate, Co[HO<sub>2</sub>C(CH<sub>2</sub>)<sub>3</sub>NH(CH<sub>2</sub>PO<sub>3</sub>H<sub>2</sub>)<sub>2</sub>]<sub>2</sub>,<sup>53</sup> the Co(II) ion in the compound was octahedrally coordinated by six phosphonate oxygen atoms from four carboxylate phosphonate ligands. While Bujoli *et al.* synthesized a 3D cobalt phosphonate,<sup>54</sup> the compound was isostructural with the pillared layered metal phosphonates M<sub>3</sub>(O<sub>3</sub>PC<sub>2</sub>H<sub>4</sub>CO<sub>2</sub>)<sub>2</sub>, M = Zn and Mn. In this structure, the magnetic transition metal ions are arranged within layers formed by the interconnection of CoO<sub>4</sub> tetrahedra and CoO<sub>6</sub> octahedra.

The strong binding ability of phosphonic acids usually lead to dense layered architectures of metal phosphonates. Incorporating other functional groups onto phosphonic linkages could improve the resultant crystallization. Different metal nodes could introduce distinct physicochemical properties into the metal phosphonate hybrid frameworks. For example, rare-earth elements would lead to photoluminescence, while magnetism was formed when cobalt was incorporated. Many other metallic precursors could also be utilized as the central ions to coordinate with phosphonic acids to obtain layered structures.<sup>55,56</sup> However, it is noteworthy that layered phosphonate hybrids often show up in the form of dense motifs. The pillars are too crowded to leave sufficient free space the interlayer region, and thus no or poor porosity is expected to be presented. A further step should be taken to generate well-

defined porosity in the phosphonate networks to make them fit the qualifications for research and practical applications.

## 2.2 Metal phosphonate materials with open-framework

A layered motif is the most common observation for a simple metal phosphonate, however, an important exception is the family of complexes observed with methylphosphonic acid. The first 3D phosphonate framework with open channels was reported in 1994 by Bujoli and co-workers.<sup>57</sup> The synthesized β-Cu(O<sub>3</sub>PCH<sub>3</sub>) contains 24-membered rings lined by pendant methyl groups. Because the distance between the opposite methyl carbons is 5.97 Å, the effective pore size is estimated at about 3 Å, which is too narrow for small adsorbate molecules such as nitrogen to enter. Thereafter, Maeda and co-workers reported the synthesis of polymorphs α- and β-Al<sub>2</sub>(CH<sub>3</sub>PO<sub>3</sub>)<sub>3</sub> with zeolite-type framework,<sup>58,59</sup> which contained trivalent aluminum cations in both tetrahedral and octahedral geometries with bridging phosphonate groups, leaving hexagonal channels lined with methyl groups, and thus giving the ~5 Å free diameter channels of both of these compounds. Then, the preparation of 3D open frameworks of metal phosphonates was fully expanded. Not only methylphosphonic acid but also methylenediphosphonic acid was used in the synthesis of open frameworks. The open-framework Co<sub>2</sub>(O<sub>3</sub>PCH<sub>2</sub>PO<sub>3</sub>)·H<sub>2</sub>O has 1D inorganic channels including 20-membered rings lined with methylene bridges.<sup>60</sup>

The phosphonate bridging moieties are almost limited to those with small organic groups such as methylphosphonate and methylenediphosphonate.<sup>33</sup> Varying the chain length in metal alkylphosphonates can alter the structures considerably. Organophosphonic linkers with -CH<sub>2</sub>- chain lengths of *n* = 2-4 typically resulted in pillared layered structures.<sup>61</sup> However, when the alkyl chain length was increased to *n* = 8, with Co<sup>2+</sup>, a low-dimensional structure resulted composed of cationic [Co(H<sub>2</sub>O)<sub>4</sub>(H<sub>4</sub>L)]<sup>2+</sup> (H<sub>4</sub>L = 1,8-octylenediphosphonic acid) chains with charge-balancing 1,8-octylenediphosphonate clathrated in the structure.<sup>62</sup> On the other hand, there are many attempts to create micropores in the open framework compounds by introducing metal oxide clusters as interlayer pillars.<sup>63,64</sup> The synthesized open framework of [NH<sub>3</sub>(CH<sub>2</sub>)<sub>4</sub>NH<sub>3</sub>]Cu<sub>3</sub>(HEDP)<sub>2</sub>·2H<sub>2</sub>O and [NH<sub>2</sub>(C<sub>2</sub>H<sub>4</sub>)<sub>2</sub>NH<sub>2</sub>]Cu<sub>3</sub>(HEDP)<sub>2</sub> (HEDP = 1-hydroxy ethylidene-1,1-diphosphonic acid)<sup>63</sup> adopts a two-dimensional layered structure with four- and eight-membered rings assembled from vertex-sharing {CuO<sub>4</sub>} units and {CPO<sub>3</sub>} tetrahedra. Co<sub>3</sub>(O<sub>3</sub>PCH<sub>2</sub>-NC<sub>4</sub>H<sub>7</sub>-COO)<sub>2</sub>·5H<sub>2</sub>O containing a proline-derived phosphonate anion has ordered micropores composed of 12 polyhedral units,<sup>64</sup> and straight 2-D channels are formed by stacking of layers. Similarly, substitution of aryl biphosphonic acid by some non-pillaring groups, such as phosphoric, phosphors, and methylphosphonic acids, could lead to the creation of interlayer pores and the increase of surface area (Fig. 1).<sup>19</sup> This method was employed to overcome the “close-pillar disposition” and resulted in a “dilution” of the phosphonate moieties. Although a porous phosphonate network can be obtained, the problem of this approach is that replacement is

random and uncontrollable, and the structural characterization and a narrow pore size distribution are still challenges. The water solubility of metal phosphonates generally decreases as the metal ion valences increase.<sup>32,65</sup> The inclusion of a second smaller “spacer” has been shown to produce porosity in tetravalent metal phosphonates,<sup>66</sup> while it often resulted in the generation of two phases when coming to divalent metal ions.

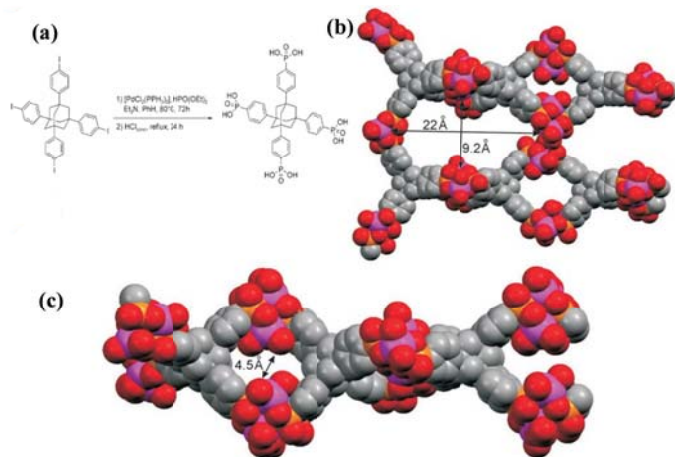


Fig. 2 Synthesis of tetrakis-1,3,5,7-(4-phosphonatophenyl)adamantane (a), and computer-stimulated model of titanium tetrakisphosphonate material (b,c).<sup>70</sup>

The study of novel open-framework or microporous metal phosphonates was accelerated by anchoring functional groups to the phosphonic linkages. A new functional group on the organophosphonate ligand would perturb the layered structure in metal phosphonates, which was hopeful for the formation of a new 3D open framework.<sup>23,31</sup> The typical functional groups attached to the phosphonic acid includes imino, pyridine, hydroxyl, carboxylic and sulfonic acid (Fig. 1).<sup>13</sup> Herein the use of bifunctional phosphonate anions and metal cations that can adopt different coordination environments is proposed as a strategy for synthesizing microporous metal phosphonates. For example, Férey and co-workers reported the open-framework lanthanide-carboxyphosphonates,  $M_4(H_2O)_7[O_2CC_5H_{10}NCH_2PO_3]_4 \cdot (H_2O)_5$  ( $M = Pr, Y$ ).<sup>67</sup> These isostructural lanthanide compounds had a three-dimensional open-framework structure and possessed a reversible hydration-dehydration capacity, demonstrating significant thermal stability up to 523 K. But the sorption data were not available. The use of amino acid derived phosphonates to form porous architectures could lead to a homochiral metal-phosphonate solid.<sup>68</sup> The chirally pure form (*S*)-proline, *N*-(phosphonomethyl)proline was reacted with a series of lanthanides to form isostructural solids, and the resultant 1D tubular channels were of  $4.32 \times 3.81$  Å free diameter. Since the introduction of pendant functional groups on the phosphonic linkers, the porosity and crystallization of the crystalline metal phosphonates are significantly perfected. From another point of view, prodigious physicochemical properties can be incorporated in the hybrid framework, thus showing a promising methodology for the crystalline growth and deep application investigation.

A large and multidimensional polyphosphonic bridging molecule would disfavour the formation of the layered motif, and thereby necessitating an open framework (Fig. 2). The organophosphonic ligand, 1,3,5,7-tetrakis(4-phenylphosphonic acid)-adamantane, was such a molecule as it possessed four phosphonic acid moieties spaced by rigid phenyl groups from an adamantane core. A number of works of metal complexes with this ligand have appeared. A vanadium phosphonate material was prepared through the non-hydrolytic condensation of vanadium(V) alkoxide with this complicated ligand, and the corresponding surface area value was  $118 \text{ m}^2 \text{ g}^{-1}$ .<sup>69</sup> The resultant porous vanadium phosphonate was testified to show favorable catalytic activity for aerobic oxidation or benzylic alcohols to aldehydes. Hybrid frameworks with titanium(IV) and this complicated and rigid ligand could be prepared as well,<sup>70</sup> indicating a paracrystalline material with  $22 \times 9$  Å pores and a high specific surface area of  $557 \text{ m}^2 \text{ g}^{-1}$ .

Hitherto, a number of strategies have been taken to improve the porosity of crystalline metal phosphonate frameworks. The main strategies can be assigned to three types, namely, using non-pillaring groups as interlayer spacers, attaching a functional group on the ligand and extending the geometry of the organic core in a polyphosphonate to direct the structure away from layered motif. Phosphonate-based MOFs have distinct differences from the carboxylate-based counterparts, such as the relatively high thermal and chemical stability and extremely low solubility, making metal phosphonates attractive candidates for porous materials. Reversely, this typically make it difficult to obtain crystalline phases with determined structures. Developments of high-throughput hydrothermal or solvothermal techniques and advances in powder XRD modeling and refinement will significantly increase the number of structurally characterized phosphonate-based MOFs, and it will be exciting to watch this field as it develops.

### 3 Mesoporous metal phosphonate materials

The dimensions and accessibility of dense or microporous crystalline metal phosphonates are restrained to the sub-nanometer scale, which confines their applications for small molecules. In parallel with the above work on dense metal phosphonates and related open frameworks, recent progress has been made towards mesoporous materials having uniform channel dimensions and pore distributions which can be adjusted over a wide range of length scales. Because of the larger pore size and pore volume of mesoporous materials in comparison with those of micropores, they have displayed superiorities in physicochemical properties and application potential. Indeed, the adaptability of the sol-gel chemistry allows the mixing of inorganic and organic components at the nanometric scale, resulting in the mesoporous organic-inorganic nanocomposites with homogeneous compositions.<sup>71</sup> This process can be accomplished in the absence or presence of surfactants, and the pore wall of the resultant solids is the assembly of hybrid nanoparticles, which is different from the covalent bonding networks of crystalline metal phosphonates.

Template-free self-assembly strategy usually initiates the assembly for the interactions among the precursor molecules, and the ordered attachment tends to form porous nanostructures.<sup>23</sup> This method does not involve the use of pre-formed templates or structure-directing agents, simplifying the preparation process. Synthesis parameters, such as the ratio of the precursors, are of significance in influencing the structural properties of the synthesized mesoporous metal phosphonates. By simply changing the ratios and the concentrations of the reagents, a series of  $\alpha$ -pillared zirconium phosphite-phosphonates with large surface area (230 to 400 m<sup>2</sup> g<sup>-1</sup>) and great pore volume (0.3 to 0.7 cm<sup>3</sup> g<sup>-1</sup>) could be obtained.<sup>72</sup> These materials showed a narrow pore size distribution that was tunable over the range 4-14 nm by varying the preparation conditions, especially the concentration of the reagents. The formation of interparticle mesoporosity was attributable to edge-edge interactions between rigid packets of a few pillared  $\alpha$ -layers giving rise to stable aggregates with a house of cards structure.

Self-assembly in the absence of structure-directing agents often involves in weak interactions among the nano-building units, including atoms, molecules and related secondary blocks, to direct the assembly process. Mesoporous metal phosphonates with well-defined porosity and nanostructures have been obtained through self-assembly strategy in the past decades. Nevertheless, this process is mainly dependent on the synthesis conditions. A more controllable method is thus required from the research and practical applications point of view.

Surfactant-assisted synthesis has been deeply and widely developed for the design of periodic mesoporous materials since 1992.<sup>73,74</sup> Rather than the individual molecule as void filler in the ordering of the reagents to form microporous hybrid frameworks, assemblies of molecules dictated by solution energetic are indispensable for the formation of the periodic pore systems.<sup>75</sup> During the synthesis process, the pre-formed surfactant micelle scaffold performs as a lyotropic liquid-crystalline phase, and subsequently the oligomers from the condensation of inorganic/organic precursors grow around the arranged micelles, leading to the assembly of an ordered mesostructured composites (Fig. 3). Removal of the surfactant by extraction or calcination can leave mesovoids in the framework. Hard-templating route have been testified to sufficiently efficient in synthesizing solid inorganic frameworks including silicas, oxides, cyanides and carbons.<sup>76</sup> However, the prepared materials often have a wider pore size distribution than that of the pristine replicas; and multiple preparation procedure at the sacrifice of the costly hard templates makes it expensive, complicated, and consequently unsuitable for large-scale production and industrial applications. Meanwhile, the template removal always involve the strong acids, bases, and high-temperature calcination, which cause it favorable for the synthesis of special mesoporous materials with solid networks including metal sulfides and oxides, carbons, and silicon carbides.<sup>23,76</sup> As to hybrid frameworks containing organic components, soft-templating approach is much more appropriate due to the modest preparation conditions to protect

the hybrid frameworks and relative simplicity, and environmental friendliness. Some typical examples of ordered mesoporous metal phosphonates are summarized in Table 1, which contains the experimental parameters, textual properties and mesophases.

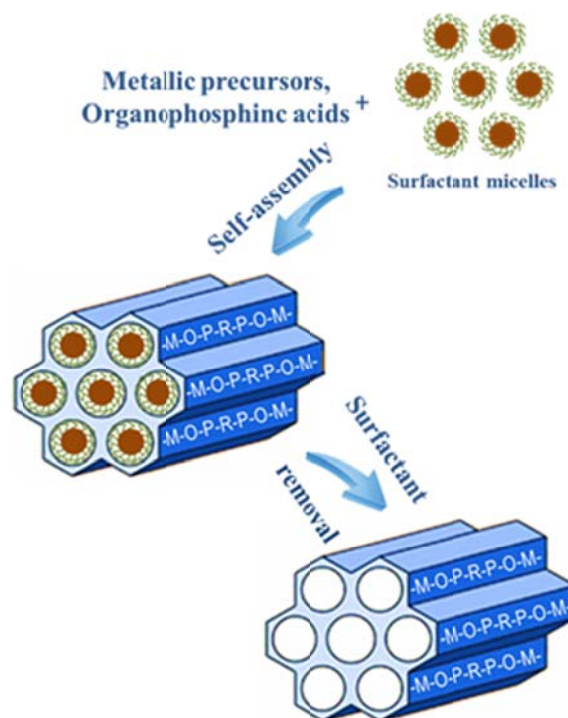


**Fig. 3** Schematic model for the formation of mesoporous metal phosphonates through soft-templating strategy.

Pure mesoporous aluminum phosphonates and diphosphonates (UVM-9) were reported by Haskouri *et al.* with organophosphorus moieties incorporated into the framework.<sup>77</sup> The resultant solids were prepared through a one-pot surfactant-assisted procedure that was based on the use of cationic surfactant (CTAB), a complexing polyalcohol (2,2',2''-nitrilotriethanol), ethylenephosphonic acid, and methylphosphonic acid or mixed phosphate/phosphonate. All materials displayed XRD patterns with at least one strong peak in the low  $2\theta$  range (associated with the [100] reflection if a hexagonal cell is assumed), characteristics of periodic mesoporous materials. TEM showed ordered mesoporous channels as well. The BET surface area of the mesoporous hybrid could reach up to 793 cm<sup>2</sup> g<sup>-1</sup> accompanied with a narrow pore width distribution around 2.7 nm. An S<sup>+</sup>T surfactant-assisted cooperative mechanism through a one-pot preparative procedure from aqueous solution was assumed. And the "atrane" complexes from the aluminum and the complexing polyalcohol were confirmed to mediate the hydrolytic rate of aluminum precursors,<sup>78</sup> thus effectively enhancing the mesoporous periodicity.

Alternatively, ordered mesoporous aluminum phosphonates could be synthesized with alkyltrimethylammonium as surfactant by the acidic strategy<sup>79,80</sup> and also with oligomeric surfactant and triblock copolymer through evaporation-induced

**Table 1** Summary of synthetic strategies and physicochemical properties of the periodic mesoporous metal phosphonates through soft-templating method.

Metallic precursor	Phosphonic acid <sup>a</sup>	Synthesis strategy	Surface area /m <sup>2</sup> g <sup>-1</sup>	Pore volume /cm <sup>3</sup> g <sup>-1</sup>	Pore size /nm <sup>b</sup>	Surfactant	Mesophase	Microstructural phase <sup>c</sup>	Ref.
Al(OBu <sup>s</sup> ) <sub>3</sub>	PDP, <i>n</i> =2	Atrane route	675	0.63	3.3	C <sub>16</sub> TABr	Hexagonal	—	66,67
Al(O <sup>c</sup> C <sub>3</sub> H <sub>7</sub> ) <sub>3</sub>	PDP, <i>n</i> =1	—	738	0.32	1.8	C <sub>18</sub> TACl	Hexagonal	—	68
AlCl <sub>3</sub>	PDP, <i>n</i> =1	EISA	788	0.44	2.2	C <sub>16</sub> TACl	Hexagonal	—	69
AlCl <sub>3</sub>	PDP, <i>n</i> =2	EISA	708	0.32	1.9	C <sub>16</sub> TACl	Hexagonal	—	69
AlCl <sub>3</sub>	PDP, <i>n</i> =3	EISA	217	0.27	3.0	Brij 58	Hexagonal	—	70
AlCl <sub>3</sub>	PDP, <i>n</i> =3	EISA	172	0.59	7.3	F68	Hexagonal	—	70
AlCl <sub>3</sub>	PDP, <i>n</i> =2	EISA	309	0.71	9.4	P123	Hexagonal	—	70
AlCl <sub>3</sub>	PDP, <i>n</i> =2	EISA	337	0.79	11.6	F127	Hexagonal	—	70
TiCl <sub>4</sub>	EDTMP	Hydrothermal and EISA	1066	0.83	2.8	Brij 56	Hexagonal	Amorphous	71
TiCl <sub>4</sub>	HEDP	Hydrothermal and EISA	1052	0.58	2.6	C <sub>16</sub> ATBr	Cubic	Amorphous	75
TiCl <sub>4</sub>	HEDP	Hydrothermal and EISA	1034	0.57	2.4	Brij 56	Hexagonal	Amorphous	132
TiCl <sub>4</sub>	EDTMP	Hydrothermal and EISA	606	0.44	2.2	Brij 56	Hexagonal	Amorphous	133
AlCl <sub>3</sub>	EDTMP	Microwave-assisted hydrothermal	498	0.61	1.7, 7.5	F127	Hexagonal	Crystalline aluminum phosphonate	119
TiCl <sub>4</sub>	EDTMP	Microwave-assisted hydrothermal	522	0.63	1.4, 7.2	F127	Hexagonal	Crystalline titanium phosphonate	119
ZrCl <sub>4</sub>	EDTMP	Microwave-assisted hydrothermal	513	0.64	1.5, 7.1	F127	Hexagonal	Crystalline zirconium phosphonate	119
VCl <sub>4</sub>	EDTMP	Microwave-assisted hydrothermal	538	0.68	1.3, 7.1	F127	Hexagonal	Crystalline vanadium phosphonate	119
Al(O <sup>c</sup> C <sub>3</sub> H <sub>7</sub> ) <sub>3</sub>	PDP, <i>n</i> =1 or 2	EISA	—	—	—	C <sub>16</sub> TACl	Lamellar	Crystalline aluminum phosphonate	72
ZrOCl <sub>2</sub>	HEDP	Hydrothermal	702	0.86	3.6	C <sub>16</sub> TABr	Wormhole-like mesopores	Amorphous	122

<sup>a</sup> PDP: Propylene diphosphonic acids, HEDP: 1-hydroxyethane-1,1-diphosphonic acid, EDTMP: Ethylenediamine tetra(methylene phosphonic acid). <sup>b</sup> The microporosity was resulted from the intraparticle aggregation. <sup>c</sup> Crystal structures have still not been defined due to the low crystallization.

self-assembly (EISA) strategy.<sup>81</sup> By using octadecyltrimethylammonium (C<sub>18</sub>TMA) based on S<sup>+</sup>I<sup>-</sup> mechanism, hexagonal mesostructured aluminum phosphonates with organically bridged diphosphonic acids ((HO)<sub>2</sub>OPC<sub>*n*</sub>H<sub>2*n*</sub>PO(OH)<sub>2</sub>, *n* = 1, 2 and 3) homogeneously distributed in the network.<sup>79,80</sup> The removal of surfactant from the as-synthesized hybrid framework has always been a difficult problem. Extraction of as-synthesized materials by acid treatment could not be achieved due to the less condensed and easily hydrolyzed frameworks. On the basis of the difference of thermal stabilities between the methylene groups of phosphonic acid and the C<sub>18</sub>TMA molecules, surfactant removal could be accessed by low-temperature calcination without decomposition of the bridged methylene groups. Oligomeric surfactants (e.g., Brij 56 and 58) or triblock copolymers (e.g., P123, F68 and F127) depending on (S<sup>0</sup>H<sup>+</sup>)X<sup>-</sup> mesostructure formation mechanism could also be

employed for the preparation of mesoporous aluminum phosphonates.<sup>81</sup> However, only simple alkyl-bridged diphosphonic acids were incorporated into ordered mesoporous phosphonate materials in these studies and the metal sources are restricted to main group metals such as aluminum.

Since different metal joints and organophosphonate linkages in the network would result in distinct physicochemical and mechanical performances, Ma *et al.* reported the periodic mesoporous titanium phosphonate (PMTP-1) material synthesized using sodium salt of ethylene diamine tetra(methylene phosphonic acid) (EDTMP) as the claw molecules with the oligomeric surfactant Brij 56 assisted in the acidic solution through (S<sup>0</sup>H<sup>+</sup>)X<sup>-</sup> surfactant-induced mechanism.<sup>82</sup> During the synthesis, a cryosol bath was used to create a low-temperature condition for slowing down the hydrolysis and condensation speeds of the reactants, and the autoclaving process was utilized and combined with the so-

called EISA method to obtain the periodic porous structure. After autoclaving at 120 °C, titanium phosphonate solution was fully condensed containing oligomeric Brij 56 micelles, followed by the EISA process under the stable temperature to give a flaxen gel (Fig. 4). The hexagonal arrangement of the mesopores could be clearly seen from TEM image with the average pore size of around 2.8 nm and the pore wall thickness of 1.8 nm. The specific surface area and pore volume of PMTP-1 were 1066 m<sup>2</sup> g<sup>-1</sup> and 0.83 cm<sup>3</sup> g<sup>-1</sup>, respectively.

Different from the synthesis of mesoporous silicas and carbons, the effective preparation of mesoporous phosphonate hybrids remains challenging, due to unmanageable reaction rate between the precursors, and the intricate interactions among the organic and inorganic components, and the surfactant micelles. However, it should be kept in mind that the key factors for the efficient assemblies to periodic mesophases include the control on the aggregation of precursors, the sufficient interactions between oligomers/precursors and surfactants, and in turn, proper size and charge of suitable building blocks.

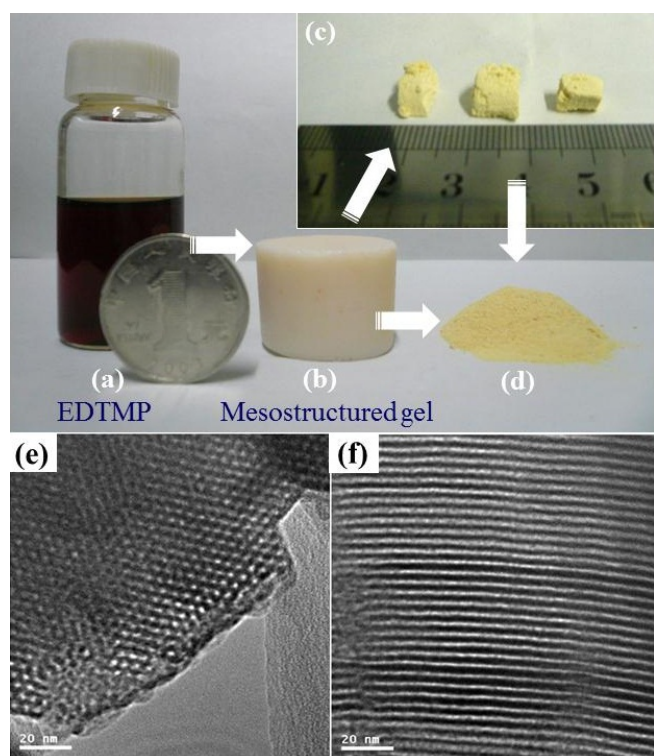


**Fig. 4** Photographs of (a) EDTMP solution, (b) as-synthesized gel before surfactant extracted, (c) mesostructured monoliths after extraction, and (d) final mashed powder. TEM images of the hexagonal mesoporous titanium phosphonate hybrid material (e,f).<sup>82</sup>

Most of the reported mesoporous metal phosphonates were of hexagonal and lamellar phases. As to lamellar phases, the removal of surfactants would lead to the irreversible collapse of mesostructures,<sup>83,84</sup> revealing the limited values from the viewpoint of practical applications. As compared with hexagonal phases, cubic mesostructures possess interconnected pore systems, showing great potential in the area of adsorption, catalysis and electronics.<sup>85</sup> Periodic cubic and hexagonal

mesoporous titanium phosphonates were first prepared using organophosphonic acid HEDP in the presence of cationic surfactant C<sub>16</sub>TAB, and the different phases of the mesopores could be transformed into each other by simply adjusting the molar ratio of the adding amount of surfactant CTAB and inorganic precursor TiCl<sub>4</sub>.<sup>86</sup> This was coincided with the previously reported molecular surfactant packing parameter theory that the hexagonal phase is formed at a low surfactant/inorganic species ratio and the cubic phase formed at a high ratio.<sup>87</sup> Interestingly, the hexagonal pore structure could be well preserved after calcination to leave purely inorganic framework, offering a new procedure to synthesize ordered mesoporous titanium phosphate materials.<sup>86</sup> However, periodic mesoporous metal phosphonates usually tend to form hexagonal mesophases. This may be due to the fact that the incompletely condensed hybrid network, the complex coordination chemistry between metal ions and organic bridges and the weak interactions among the organic components may devote to forming relatively stable hexagonal phases.

On the other hand, the pore size is mainly dependent on the hydrophobic portions of the soft-templating molecules (Table 1). The pore size increased with the hydrophobic volume, admitting the adjustment of pore width at the nanometer scale. In general, the resultant pore size distributes in the region of 2-4 nm for ionic and oligomeric surfactants with low molecular weight,<sup>77-81</sup> 6-10 nm for some Pluronic block-copolymers,<sup>81</sup> even large mesopores (30 nm) when using polystyrene-*block*-poly(oxyethylene) colloidal template.<sup>88,89</sup>

Each synthesis pathway has its own advantages and disadvantages. EISA method can fit wide preparation conditions owing to the alleviated hydrolysis speed of metallic precursors, though this strategy needs relatively rigorous conditions including temperature and humidity. Hydrothermal autoclaving process is a quick and efficient route, though the energy consumption is required for the high temperature and pressure. One should choose the most suitable pathway depending on the practical situation. Exploring low-cost, environmentally friendly and reproducible method is still urgent.

The syntheses of disordered wormhole-like mesoporous metal phosphonates templated by supermolecular surfactants have also contributed a great deal to the exploiting of the organization principles in the surfactant-assisted strategy. Disordered mesostructures have no unit cell, symmetry and space group. Although the resultant mesostructures are disordered, uniformly sized mesopores, high surface area and easy modulation can usually be achieved, offering them potential in catalysis, adsorption, separation and immobilization. Due to the complexity, it is still difficult to pass a definitive verdict to which kind of mesostructures are more benefit in applications, disordered or ordered. The territory of preparing mesoporous phosphonate-based hybrids has not been exploited as mature as the silicas and carbonaceous materials owing to the complex interconnected factors, coordination and sol-gel chemistry. Thus further investigation endeavors should be of significance and invested subsequently.

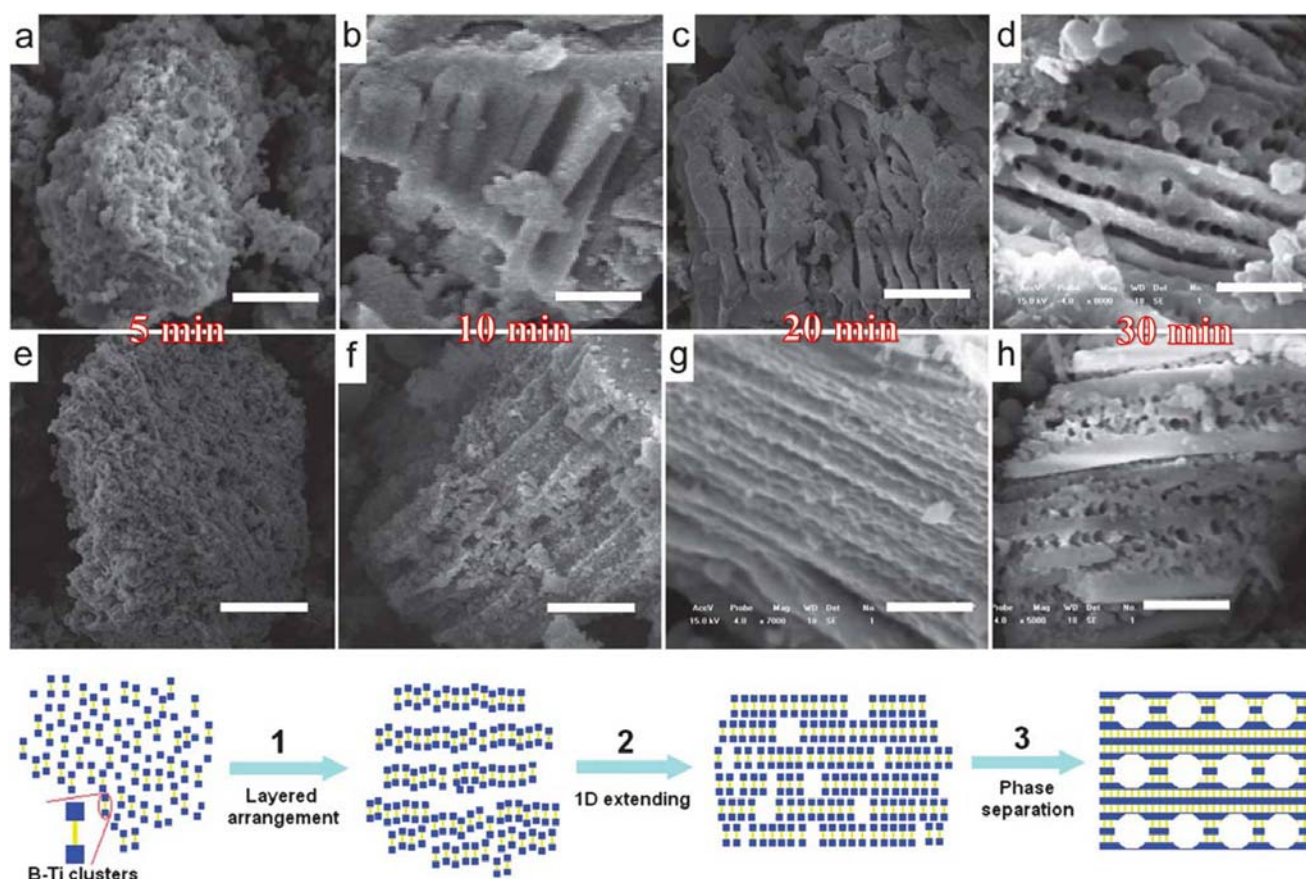


Fig. 5 Time-dependent SEM images of hierarchical porous titanium phosphonates with P/Ti = 1/4 (a-d) and 1/2 (e-h), scale bar: 2  $\mu\text{m}$ . And a proposed formation mechanism for the obtained macrostructures.<sup>36</sup>

#### 4 Metal phosphonates with hierarchical porosity

Hierarchical materials containing interconnected porous structures have enhanced properties compared with single-sized pore materials due to increased mass transport through the material and maintenance of a specific surface area on the level of fine pore systems.<sup>90</sup> Thus, extended performances from adsorption/separation to shape-selective catalysis and biology could be perceived.<sup>91</sup> Metal phosphonates with hierarchical porosity (micro-/mesoporosity and meso-/macroporosity) are summarized and tabulated in Table 2.

Self-assembled crystalline metal phosphonates could lead to bimodal porosity, intracrystalline micropores and interparticular mesovoids.<sup>92,93</sup> Furthermore, hybrids with self-assembled nanostructures and hierarchical porosity are highly desirable in the context of heterogeneous catalysis. Macropores or macrovoids could be created by using either hard or soft templates, such as colloidal crystals,<sup>94</sup> emulsions,<sup>95</sup> and polymers,<sup>96</sup> or through a spontaneous process in the absence of any surfactants.<sup>97</sup> For example, an inverse opals method could be applied to prepare a three-dimensionally ordered macroporous titanium phosphonate material.<sup>98</sup> The synthesized titanium phosphonate presented a 3D-ordered arrangement of interconnected macropores with a mean pore diameter of 400

nm, which was *ca.* 10-15% smaller than the size range of original PS spheres templated, suggesting significant shrinkage during latex sphere extraction. Although templating method is efficient and general, the further removal of the templates not only perplexes the fabrication procedures, but also may result in the collapse of the structures, and even detrimentally introduce some impurities. Thus a hierarchical architecture through a simple approach with both mesopores and macropores is expected, which could combine the superiorities of the porosity at two scales.

Microemulsion-mediated method has testified effectively used to prepare meso-/macroporous materials,<sup>99,100</sup> as well as metal phosphonates.<sup>101</sup> Uniformly arranged macroporous channels (100-300 nm) were composed of mesostructured porous walls. Wormhole-like mesopores of 2.5 – 5.8 nm in size presented in the vicinity of the surface, which is accompanied with a new mesocellular foam structure (8 – 10 nm) in the core region. Since the titanium tetrabutoxide rapidly hydrolyzed in the EDTMP solution, nanometer-sized titanium phosphonate form immediately with butanol molecules as byproducts. Thus, microemulsion drops formed in the multicomponent system composed of alkoxide-organophosphonate-alcohol-water. The phosphonate sols aggregated along with the microemulsions, evolving to mesocellular foam structure. The interactions between the sols caused the formation of mesostructured

**Table 2** Summary of synthetic parameters and physicochemical properties of the hierarchical porous metal phosphonates.

Porous hierarchy	Metal sources	Phosphonic acids <sup>a</sup>	Pore size /nm <sup>b</sup>	Surface area /m <sup>2</sup> g <sup>-1</sup>	Pore volume /cm <sup>3</sup> g <sup>-1</sup>	Surfactant	Crystallization	Ref.
Micro- /Mesoporosity	SnCl <sub>4</sub>	BTPA	1.3,3.5	380	0.16	—	Hexagonal crystal phase	81
	NiCl <sub>2</sub>	HDTMP	1.3,—	241	0.29	—	Tetragonal crystal phase	82
	SnCl <sub>4</sub>	Phytic acid	1.5,2.5	347	—	—	Low crystallization	120
	FeCl <sub>3</sub>	BTPA	1.1,2.6	556	0.029	—	Triclinic crystal phase	121
	SnCl <sub>4</sub>	BDC	1.2,2.6,6.8	338	0.54	—	Tetragonal crystal phase	124
	SnCl <sub>4</sub>	PEHMP	1.4,2.9,4.8	723	0.87	C <sub>16</sub> TABr	—	125
Meso- /Macroporosity	Ti(O <sup>n</sup> Bu) <sub>4</sub>	EDTMP	2.5-10,100-300	86	0.074	—	Amorphous	90
	Ti(O <sup>n</sup> Bu) <sub>4</sub>	HEDP	2.0,90-400	257	0.263	—	Titania-phosphonate	91
	Ti(O <sup>n</sup> Bu) <sub>4</sub>	ATMP	4.9,50-100	323	0.22	—	Amorphous	92
	Ti(O <sup>n</sup> Bu) <sub>4</sub>	BHMTMP	4.8,400-600	307	0.21	—	Amorphous	96
	Ti(O <sup>n</sup> Bu) <sub>4</sub>	DTPMP	5.1,500-1000	269	0.22	—	Amorphous	123
	Ti(O <sup>n</sup> Bu) <sub>4</sub>	HEDP	2-3,800-1200	511	0.67	P123	Amorphous	95
	Al(O <sup>n</sup> C <sub>3</sub> H <sub>7</sub> ) <sub>3</sub>	ATMP	5.4,500-2000	154	0.44	F127	Amorphous	97
		BHMTMP	5.0,500-2000	128	0.42	F127	Amorphous	97

<sup>a</sup> HDTMP: hexamethylenediamine-*N,N,N',N'*-tetrakis-(methylphosphonic acid), BTPA: benzene-1,3,5-triphosphonic acid, BDC: butylene-1,4-diphosphonic acid, PEHMP: pentaethylenhexamine-octakis-(methylphosphonic acid) hexadecadosodium salt, ATMP: amino tri(methylene phosphonic acid). <sup>b</sup> Micro- and mesoporous size are calculated from the N<sub>2</sub> sorption isotherm, and the macropore size distributions are determined from the observation of electron microscopy.

nanoclusters of several nanometers in size. If 1-hydroxyethylidene-1,1-diphosphonate was chosen as organic precursors, according to microemulsion methodology, the interfacial polymerization of titanium phosphonate sols and titanium-oxo clusters resulted in the formation of mesostructured hybrid nanorods with a length of 80 – 105 nm and a thickness of 18 – 38 nm.<sup>102</sup>

Interestingly, organic additives could be utilized to create macropores in the mesoporous hybrid substrates. By using  $\beta$ -cyclodextrin as an organic additive, well-structured mesopores were produced from worm-like cyclodextrin aggregates.<sup>103,104</sup> Additionally, large spherical pores with sizes between 50 – 100 nm were found among the wormhole-like mesopores, which could be the inverse spaces of spherical cyclodextrin aggregates.<sup>105</sup> It is noteworthy that the pH condition of the reaction system influences the hydrolysis rate of inorganic metallic precursors tremendously. Too high pH value would cause the rapid hydrolysis rate, which thus disrupted the microphase separation process and led to poor porosity. However, when the pH value was further lowered to improper

acidic range, the newly formed metal phosphonate clusters would be partially dissolved, resulting in poor structured porosity and incompletely condensed framework. Consequently, moderate pH condition was found to be vital in obtaining hierarchical porous phosphonates with stable hybrid networks.

A mild solvent evaporation strategy was used to synthesize titanium phosphonate hybrid materials with a hierarchically meso-/macroporous structure in which copolymers F127 and P123 were used as structure-directing agents and HEDP as phosphonic linker.<sup>106</sup> All the samples possessed a macroporous morphology of the mesoporous framework, resulting in high surface areas (> 370 m<sup>2</sup> g<sup>-1</sup>). Noticeably, mesostructured titanium phosphonates with unusual uniform lines of macropores were synthesized by using bis(hexamethylenetriamine) penta(methylenephosphonic acid) (BHMTMP) as the coupling molecule, through a one-pot hydrothermal process without any surfactant assistance (Fig. 5).<sup>96</sup> A wormhole-like mesostructure and many uniform parallel lines of macropores were divided by solid ridges in the same direction. This novel macropore architecture has never been



investigated.<sup>112</sup> It was found that the monolayers of  $C_{18}H_{37}P(O)(OH)_2$  demonstrated the better hydrolytic stability than other cotadecyl organosilane modifiers. High stability of these phosphonate monolayers is explained because of strong specific interactions of phosphonic acid group with the surfaces of metal oxides. On the basis of the above mentioned works, the feasibility of grafting phosphonic acids onto metal oxides is fully confirmed. Soler-Illia *et al.* prepared organic modified transition-metal oxide mesoporous thin films and xerogels by using dihexadecyl phosphate (DHDP), monododecyl phosphate (MDP) and phenyl phosphate (PPA).<sup>113</sup> Dramatic differences were observed for the incorporation of organophosphonates in mesoporous versus nonmesoporous solids, demonstrating that the organic functions were incorporated inside the pore system. Incorporation behaviors were also observed depending on the mesostructure; cubic 3D mesostructures are more accessible than their 2D hexagonal counterparts.<sup>114</sup> Furthermore, the functionalized pores were found to be further accessible to other molecules (solvent, fluorescent probes) or ions (*i.e.*,  $Hg^{2+}$ ), opening the way for sensor or sorption applications.

Besides the monophosphonic acids mentioned above, Yuan and co-workers reported the use of a series of amine-based organophosphonic acids and their salts as organophosphorus coupling molecules in the one-step synthesis and the application exploration of the oxide-phosphonates and metal organophosphonate hybrid materials with mesopores and hierarchically meso-/macroporous architecture.<sup>115,116</sup> Claw molecules of ethylene diamine tetra(methylene phosphonic acid) and diethylene triamine penta(methylene phosphonic acid) were anchored to the titania network homogeneously. The synthesized titania-phosphonate hybrids showed irregular mesoporosity formed by the assembly of nanoparticles in a crystalline anatase phase. The synthesis process is quite simple in comparison with the previously reported two-step sol-gel processing involving first the formation of  $P-O \cdots M$  bonds by non-hydrolytic condensation of a metal alkoxide with a phosphonic acid and then the formation of the  $M-O-M$  bonds of the metal oxide network by hydrolysis/condensation of the remaining alkoxide group.<sup>8</sup> The burdensome work to remove the residual organic solvent was not needed.

Phosphonic acids can bind strongly to a wide variety of metal oxides, and even metals, sulfides, nitrides. On one hand, the original physicochemical properties of the bulk materials can be preserved. On the other hand, diverse phosphonates with novel specialities including bioactivity, electronic conductivity and photochemical properties can be incorporated, showing the capacity to be further modified as well. Furthermore, the phosphonic ligand are not sensitive to moisture and do not polymerize with each other, thus presenting facile and robust procedures for deposition of dense and homogeneous phosphonate layers.

## 6 Potential applications

Applications for inorganic-organic metal phosphonate hybrid materials are emerging. Owing to their extremely plentiful

porosity, adjustable compositions, controllable structures, metal phosphonates have been developed as multifunctional materials to display versatile excellent performances beyond the traditional use as catalysts and adsorbents, even contributing to the developments in the fields ranging from energy storage and conversion to medical diagnosis and therapy. In this section, the typical and emerging applications of metal phosphonates are highlighted and discussed.

### 6.1 Multiphase adsorption and separation

The capture of green-house gases such as carbon dioxide ( $CO_2$ ) under practical conditions is quite significant because of the implications for global warming, and the removal of  $CO_2$  from industrial flue gas has become an important issue. Among a number of  $CO_2$  capture solids including porous carbons,<sup>117,118</sup> amine-modified mesoporous silicas,<sup>119</sup> carbon-CaO nanocomposites,<sup>120</sup> and carboxylate-based MOFs,<sup>121</sup> phosphonate-based MOFs exhibiting certain advantages such as high surface area, large pore volume, uniform pore width, low cost and relatively high stability are promising for  $CO_2$  capture over a wide range of operating conditions.  $Cu(1,4$ -benzenediphosphonate bis(monoalkyl ester) isomorphous framework with an methyl tether could capture  $CO_2$  with a high isosteric heat of adsorption of  $45 \text{ kJ mol}^{-1}$ ,<sup>122</sup> and a modest uptake of  $CO_2$  at ambient temperature was observed, 6.06 wt% at 273 K and 1200 mbar. The phosphonate monoesters could balance crystallinity and permanent porosity that was accessible to  $CO_2$ . Using a triazole modified phosphonate ligand, 4-(1,2,4-triazol-4-yl)phenylphosphonic acid), could result in high selectivity for  $CO_2$  over  $N_2$  (114 : 1),<sup>123</sup> which might be due to that the higher polarizability and quadrupole moment of  $CO_2$  compared with  $N_2$  caused a higher affinity of the pending polar functionalities ( $-PO_3H^{-1}$ ) within the channels. The resultant  $CO_2$  uptake amount was 15.8 wt%.

Recent theoretical and experimental studies have revealed the correlation between the amount of  $CO_2$  adsorbed and the surface area or pore volume, as well as the increase of adsorption enthalpy for the host materials with open metal sites and active organic functionalities.<sup>117,124</sup> In particular, the incorporation of mesoporosity and even hierarchical porosity can optimize the adsorption capacity and kinetics. The  $CO_2$  adsorption equilibrium for meso-/macroporous titanium phosphonates could be reached within 50 min.<sup>107</sup> The  $CO_2$  uptake was  $0.89 \text{ mmol g}^{-1}$  at  $40 \text{ }^\circ\text{C}$ , which was higher than some pure silica adsorbents ( $0.52 \text{ mmol g}^{-1}$ ) with specific surface area up to  $900 \text{ m}^2 \text{ g}^{-1}$ .<sup>125</sup>

It is noteworthy that the adsorption capacity of porous metal phosphonates remained stable even after multiple cycles, making them promising in practical applications.<sup>106</sup> Increasing the  $CO_2$ -framework interactions and improving the porosity of the phosphonate hybrid frameworks present the major challenge and bottleneck in capturing  $CO_2$ . Creating open metal sites and introducing basic sites have been shown to effectively increase the interactions. Moreover, in comparison with the carboxylate-based MOFs, the storage of fuel gases such as hydrogen and methane on porous metal phosphonates is

scarcely reported. Rigorous investigation towards highly stable and affordable metal phosphonates for theoretical research and practical applications is urgently needed.

Adsorption from liquid phase is much more complicated compared with gas phase adsorption due to the competitive behaviors between solute and solvent for the solid surface. The adsorption of a solute is mainly dependent on the molecular sizes and physicochemical properties, and on the textural properties and surface chemistry of an adsorbent. It can be envisioned that metal phosphonates can perform as good adsorbents for the removal of heavy metal ions from waste waters, due to that the organic functionalities serve the formation of complexes with metal ions through acid-base interactions, and the easy separation of the loaded solid adsorbent from liquid phase are preferable. For instance, the coupling organophosphonic molecules were homogeneously incorporated into the mesoporous walls of the titanium phosphonate PMTP-1 materials, and the specific structure of ethylenediamine could chelate metal ions.<sup>82</sup> The maximum adsorption capacity based on Langmuir isotherm model was determined to be 36.49, 29.03, and 26.87 mmol g<sup>-1</sup> adsorbent for Cu<sup>2+</sup>, Pb<sup>2+</sup>, and Cd<sup>2+</sup>, respectively. Further experiments confirmed that, besides the ethylenediamine groups, other electronegative groups or atoms including -OH, -SH, and N, could contribute to metal ion adsorption. Meanwhile, the adsorption characteristics of organic pollutants on mesoporous metal phosphonate materials were also identified. It is revealed that mesoporous titanium phosphonate PMTP-1 exhibited excellent adsorption performance for the cationic dye methylene blue (MB) as target pollutant from aqueous solution.<sup>126</sup> The adsorption equilibrium was achieved after 30 min of contact time, and the adsorption of MB on PMTP-1 was best fitted to the Langmuir isotherm model with the maximum monolayer adsorption capacity of 617.28 mg/g, indicating that the PMTP-1 could be used as an efficient adsorbent for the removal of textile dyes from effluents.

The adsorption of biomacromolecules such as proteins from solution onto solid surfaces is also of great scientific importance in many areas, such as biology, medicine, biotechnology and food processing.<sup>127</sup> Under pH conditions close to the isoelectric point, the adsorption of lysozyme on aluminum phosphonate hybrid materials was dominated by host-guest hydrophobicity-hydrophobicity interactions.<sup>108</sup> Interestingly, unlike inorganic-framework adsorbents used for adsorption of proteins,<sup>128</sup> the porous phosphonate hybrid adsorbents had an organic-inorganic framework, which contains plenty of hydrophobic alkyl groups inside the framework.<sup>108</sup> The hydrophobicity/hydrophilicity could be controlled at a chemical dimension. So the hydrophobic interaction between the organic groups inside the channel walls and the nonpolar side chains of the amino acids on the surface of lysozyme was greatly enhanced, leading to the increased monolayer adsorption capacity. When extra-long hydrophobic alkyl chains (-[CH<sub>2</sub>]<sub>6</sub>-) was incorporated, the resultant adsorption ability was higher than that synthesized with organophosphonate of lower hydrophobic -CH<sub>2</sub>- groups. Since

various biomolecules exhibit distinct isoelectric point and spatial sizes, thus the molecules can be effectively adsorbed and separated by changing pH conditions, and the porosity and pore structures of metal phosphonates.

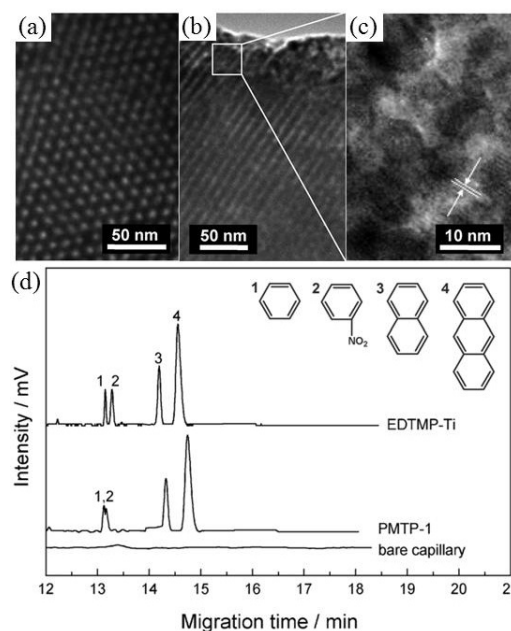


**Fig. 7** TEM images of hexagonal mesoporous titanium phosphonate (a,b,c), and OTCEC separation of neutral compounds at pH = 3.0 (d). PMTP-1 and EDTMP-Ti stand for amorphous<sup>82</sup> and crystalline<sup>130</sup> ordered mesoporous titanium phosphonates, respectively.

Chromatography (*e.g.*, gas- and liquid-phase) is one of the most powerful separative methods in analytical chemistry. PMOs and organically modified mesoporous silicas have been demonstrated as the stationary phases in reverse-phase high-performance liquid chromatography (HPLC) in the form of packed columns, for the separation of only neutral compounds.<sup>90,129</sup> However, packed columns usually result in low resolution as a result of peak broadening, which impairs the separation efficiency of these hybrid materials. Recently, a series of hexagonal periodic mesoporous metal phosphonates with semi-crystalline pore walls synthesized by microwave irradiation were firstly employed as the stationary phase in the open-tubular capillary electrochromatography (OTCEC) separation technique,<sup>130</sup> which combines the efficiency of capillary electrophoresis and the selectivity of HPLC. The presence of functional groups inside the framework and the excellent properties of the obtained metal phosphonates, including well-ordered pores with large surface area and pore volume and high thermal stability, could improve selectivity and so encouraged their use as the stationary phase in wall-coated OTCEC separation for various substances including acidic, basic, and neutral compounds. In the case of neutral compounds including benzene, nitrobenzene, naphthalene, and anthracene (Fig. 7), the elution order was benzene < nitrobenzene < naphthalene < anthracene on the mesoporous titanium phosphonate coated capillary, suggesting a hydrophobicity mechanism for the separation of the species.

For contrast, for the ordered mesoporous titanium phosphonate constructed from the same phosphonate linkers (EDTMP) but with an amorphous framework, benzene, naphthalene, and anthracene could be well separated, while benzene and nitrobenzene could not be completely separated. This indicated that, in addition to hydrophobic interactions, suitable polarization of the crystalline mesoporous phosphonates was responsible for the effective separation of benzene and nitrobenzene. Since the separation efficiency mainly depends on the host-guest interactions between stationary and mobile phases, such as hydrophobicity-hydrophobicity interaction, polarity, and intermolecular forces, phosphonate hybrid materials, constructed by long alkyl chains,<sup>108</sup> multidimensional linkages,<sup>69,70</sup> or phosphonic linkers with polar pendant groups,<sup>30,32</sup> can also be used in chromatography technique, and it is worth exploring.

Although porous metal phosphonates have been successfully applied in adsorbing CO<sub>2</sub>, toxic metal ions and organic contaminants, and separating organic compounds, some further studies are still needed to illustrate the host-guest interactions, such as model fitting and calculation analysis, supplying theoretical basis to direct synthesis and to optimize the adsorption/separation capabilities. Thus it is believed that metal phosphonates will find their real value in adsorption and separation in near future.

## 6.2 Catalysis

The exploration of porous metal phosphonates as heterogeneous catalysts is considerably interesting due to the wonderful porosity that is favorable for the diffusion of reactants and products. And it is possible to tailor the porous structures and functionality to yield the chemo-, regio-, stereo- and/or enantioselectivity by creating an appropriate environment around the catalytic center in the restricted space available. Furthermore, owing to the homogeneous compositions of hybrid frameworks, a homogeneous distribution of active sites can thus be envisioned.

### 6.2.1 Pure hybrid frameworks

As an attractive alternative to reduce the consumption of fossil fuels, biodiesel is renewable, biodegradable and can be synthesized by transesterification of triglycerides or esterification of free fatty acids. Typically, the practical industrial production involves homogeneous acid (*e.g.*, concentrated sulfuric acid) and alkaline catalysts, which are of serious environmental concern and pose difficulties in separation and purification of the target products. Recently, mesoporous tin phosphonate hybrid monolith was used to catalyze the esterification of long chain fatty acids with methanol under mild conditions.<sup>131</sup> As an example, the catalyst showed excellent catalytic activity at room temperature and 94% isolated yield was obtained for lauric acid. The catalytic activity showed negligible loss after five times recycles. Supermicroporous iron phosphonate with interparticular mesoporosity found potential in transesterification reactions

under solvent-free conditions.<sup>132</sup> The electrophilicity of the carbonyl carbon of the reactant ester group was the main driving force of the reaction. Negatively charged free P-OH in the porous framework could prevent molecules enriched with  $\pi$ -electron clouds from entering the porous channels. Thus, the  $\pi$  electrons could be responsible for the minimal conversion of ethyl acrylate to the corresponding transesterified product in comparison with the other targeted esters. After the fifth cycle, the yield of methylcyanoacetate decreased slightly to 85.6 %, compared with 88.9 % in the first run, indicating the stability of the catalytic activity. The catalytic stability after multiple cycling could be due to the stability of Me-O-P bond, leading to the solid hybrid phosphonate frameworks and no leaching of active components during reaction process.

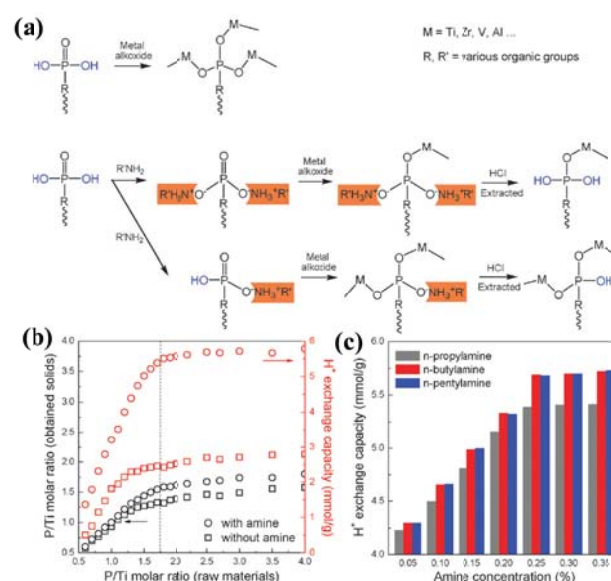


**Fig. 8** Alkyl amine-assisted preparation of titanium phosphonates (a), the P/Ti molar ratios (b) and ion-exchange capacity (c) of the resultant titanium phosphonates.<sup>134</sup>

Acid content is one of the key elements to determine catalytic activity and efficiency. Mesoporous zirconium organophosphonate, possessing a specific surface area of 702 m<sup>2</sup> g<sup>-1</sup> and a uniform pore size of 3.6 nm, was synthesized with the assistance of C<sub>16</sub>TAB using HEDP as coupling molecule.<sup>133</sup> It was confirmed the existence of defective P-OH, showing ion exchange capacity of 1.65 mmol g<sup>-1</sup>. The resultant hydroxyethylidenebridged mesoporous zirconium phosphonate could serve as acid catalyst for the synthesis of methyl-2,3-O-isopropylidene- $\beta$ -D-ribofuranoside from *D*-ribose, exhibiting high catalytic activity with rapid reaction rate (a product yield of 35.6% after reaction at 70 °C for 3 h), which were comparable to the catalytic performance of liquid acid HCl (yield of 26.2%) or commercial ion-exchange resin (yield of 33.0%). The excellent catalytic activity could be attributable to the high surface area of the synthesized mesoporous zirconium phosphonates. The high specific surface area is beneficial for the distribution of the active sites and for their exposure so that

they can readily be attached by the reactants, and the mesopores aid in the acceleration of mass transfer.

Nonetheless, it was difficult to access high acidic content of the metal phosphonates during the conventional synthesis methods, since the condensation between P–OH and metal ions during the preparation process often results in the extensive formation of P–O–Me (Me = Ti, Zr, V, Al, *etc.*) bonding mode instead of defective P–OH. In order thus to increase the defective P–OH concentration in metal phosphates and phosphonates for the improvement of the H<sup>+</sup> exchange capacity, a series of alkyl amines could be used as protective groups during the condensation process, based on the reversible reaction between alkyl amines and P–OH groups in the phosphonic bridging molecules (Fig. 8).<sup>134</sup> This alkyl amines first partially occupied P–OH sites by acid-base reactions, followed by the condensation between the added alkoxides and residual P–OH and P=O groups. And the extraction with HCl would finally release P–OH defects of the resultant solids, leading to the high H<sup>+</sup> exchange capacity and acid content. In the absence of amines, the P/Ti ratio reached a plateau of 1.35–1.51 when the added P/Ti ratio was larger than 1.75, due to the limit of coordination ability of Ti<sup>4+</sup> ions with phosphonic acids. In the presence of amines, the P/Ti ratio of obtained solids exhibited a sharp initial rise, and finally reached a plateau of 1.59–1.80, which was higher than that without amines added. Correspondingly, a similar tendency could be observed for H<sup>+</sup> exchange capacity of the synthesized materials. The highest H<sup>+</sup> exchange capacities could be confirmed as 2.44–2.79 and 5.51–5.80 mmol g<sup>-1</sup> for the samples synthesized without and with amines assistance, respectively. High yield of 48.7% for methyl-2,3-*O*-isopropylidene- $\beta$ -*D*-ribofuranoside could be achieved. The product yield was hardly decreased even after 10-time reuse.

Tetragonal tin phosphonate hybrid with mesoscopic voids, synthesized by using diphosphonic acid as spacers, could be employed as catalyst for the polymerization of styrene to polystyrene in the absence of solvent, and for partial oxidation of styrene to phenylacetaldehyde and acetophenone in the presence of various aprotic solvents with dilute aqueous H<sub>2</sub>O<sub>2</sub> acted as an initiator/oxidant.<sup>135</sup> The polymerization could be finished at room temperature within 2–3 h reaction time. But the BET surface area of tetragonal tin phosphonate was relatively low (338 m<sup>2</sup> g<sup>-1</sup>). By using CTAB as structure-directing agent, the surface area of tin phosphonate could be increased to 723 m<sup>2</sup> g<sup>-1</sup>, accompanied with micropores due to crosslinking of the ligand.<sup>136</sup> This hybrid demonstrated excellent catalytic activity in direct one-pot oxidation of cyclohexanone to adipic acid using molecular oxygen under liquid phase conditions. The tin in the framework activated the molecular oxygen, helping to form the cyclic six-membered transition state, which further rearranged into a cyclic ester.

CO<sub>2</sub> can serve as C1 building block for various organic chemicals. One of the most promising reaction schemes currently seems to be the formation of cyclic carbonate *via* coupling of CO<sub>2</sub> and epoxides, which are useful as monomers, solvents, and pharmaceutical/fine chemical intermediates, and

in biomedical applications.<sup>137</sup> Carboxylate-based MOFs have been extensively studied in this area.<sup>138–142</sup> Song *et al.* reported the coupling reaction of CO<sub>2</sub> with propylene oxide to produce propylene carbonate catalyzed by MOF-5 in the presence of quaternary ammonium salts.<sup>138</sup> The synergetic effect between MOF-5 and quaternary ammonium salts had excellent effect in promoting the reaction. The cycloaddition of CO<sub>2</sub> with epoxides is considered to be catalyzed by basicity and promoted by the Lewis acidic sites. On the basis of the intrinsic catalytic sites of the metal-connecting points (weak Lewis acid), the introduction of basic amino groups could lead to the enhanced catalytic performance.<sup>142</sup> Bifunctional hybrid catalysts containing moderate Lewis acidic and basic sites are preferred in the cycloaddition reactions. The bifunctionality can not only enhance the conversion and selectivity, but also can simply the reaction conditions. The attempted bifunctionality can be obtained through judicious selection of precursors or through pre- and post-modification of the organic linkers. Up to now, reports concerning metal phosphonates for the coupling of CO<sub>2</sub> and epoxides are relatively scarce. Since metal phosphonates show the similar characteristics of compositions and structures and higher stability compared to the carboxylate counterparts, it is quite significative to explore the catalytic activity of metal phosphonates in this burgeoning area.

### 6.2.2 Post-functionalization for catalysis

Chemically designed ordered mesoporous titanium phosphonate hybrid materials have exhibited the capacity to be functionalized by sulfation with chlorosulfonic acid (ClSO<sub>3</sub>H) to form stable hydrosulfated esters.<sup>143</sup> The specific alkyl hydroxyl structure of the coupling molecule HEDP makes its sulfation facile. Approximately 2.69 and 3.93 mmol g<sup>-1</sup> of H<sup>+</sup> were assigned to the grafted sulfonic groups and the defective P–OH from the hybrid framework, respectively. The acid strength revealed a Hammett indicator of  $H_0 < -11.35$ , indicative of a strong solid acid. It was also proven that the hydrosulfated groups remained at the pore walls even in hot water (up to 80 °C), which allowed the functionalized sample to be used as an ion exchanger and acid-base catalyst in room or low temperature reactions. For example, the sulfated materials could be used in the esterification of oleic acid and methanol under ambient temperature and pressure, giving a much higher conversion (87.3%) than the unfunctionalized materials (4.9%).

Inspired by the Langmuir adsorption behavior of metal ions onto porous phosphonates,<sup>82,86</sup> a step further would transform the metal ions into active components, which could find possible potential in some catalytic reactions. To achieve the high dispersion of CuO nanoparticles, the Cu<sup>2+</sup> ions were firstly coordinated on the metal phosphonate material in the form of monolayer behaviour, and a subsequent calcination at 450 °C would generate the highly dispersed CuO active components.<sup>144</sup> Since the PMTP-1 microspheres was thermally stable to 450 °C, the high temperature calcination could realize the high dispersion of CuO while maintain the mesoporous hybrid framework. The density and distribution of the surface organic functional groups could be tuned, allowing for an indirect

adjustment of the dispersion of the  $\text{Cu}^{2+}$  and the final CuO loading amounts. A main reduction peak at 217 °C was observed in the temperature-programmed reduction ( $\text{H}_2$ -TPR) analysis of the synthesized catalysts, which was lower than that of pure CuO and CuO catalysts supported on inorganic metal phosphates without organic ligands (252 °C). It is commonly accepted that a high dispersion of active components on the supports can contribute to improving the catalytic oxidation performance.<sup>145</sup> The oxidation of toxic CO was selected as probe reaction, and the catalytic activity of the synthesized supported catalyst was higher than those of materials with the same CuO content but prepared by the conventional impregnation methods. Moreover, the synthesized catalyst showed a significant stability for low-temperature CO catalytic oxidation.

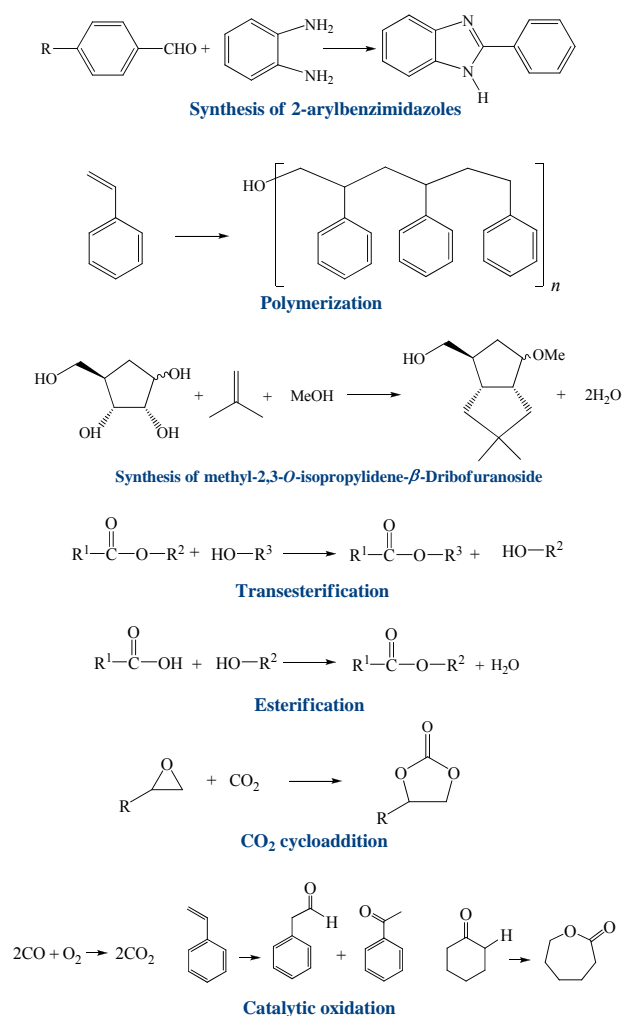


**Fig. 9** Summary of some emerging and potential catalytic applications of metal phosphonates.

Noble metals, such as Au, Ag, Pt and Pd, have been known for their outstanding catalytic performances. Encapsulation of noble metal nanoparticles inside the metal phosphonate frameworks may extend applications in catalysis and energy conversion by catalytic spillover.<sup>146,147</sup> Interestingly, the

precious nanoparticles with different size regimes could be made through different reduction method, reduction in ethanol (10-15 nm) and at elevated temperature under hydrogen (2-4 nm).<sup>146</sup> This provides a simple way to control the size of the loaded active components.

Catalytic reactions are indeed surface interaction processes, where the metal joints and organophosphonate bridging groups perform as active sites. The special compositions and a variety of structural features can engender catalytic activity in metal phosphonates (Fig. 9). Post-modification can mainly be based on the organic motifs inside the framework, which can create novel physicochemical properties, such as acidity/alkalinity, hydrophobicity/hydrophilicity, chirality. However, they are still confronted with issues concerning thermal stability and chemical robustness, due to the nature of the components of the materials. Catalysis on the basis of metal phosphonates is still at its infancy.

### 6.3 Energy conversion and storage

With the rapid development of modern society, energy issue has received increasing attention. On the basis of the ever-increasing demand for clean energy, environmentally sustainable energy resources are urgently needed, and renewable solar energy is regarded as an alternative to conventional fossil fuels. Moreover, there has been significant interest in the development of alternative electronic devices.

#### 6.3.1 Solar energy utilization

By introducing specific functional groups into the metal phosphonate material, photochemical and photoelectric energy conversion can be realized. Photocatalytic process is representative of the utilization of solar energy.  $\text{TiO}_2$  is the most studied photocatalyst for environmental remediation and energy conversion. However, pristine  $\text{TiO}_2$  with unfavorably large band gap usually exhibits a low quantum yield. Foreign-element doping is an effective approach to extend the light adsorption range and to reduce the recombination of photo-generated carriers. On the other hand, titanium phosphonates can be considered to be potential photocatalysts, due to phosphonic incorporation into titania framework.<sup>86,98,101</sup> The homogeneous doping (*e.g.*, C, P, and N) of titanium phosphonates network from the bridging molecules and well-structured porosity could increase the photoadsorption efficiency and enhance the mass transfer. Correspondingly, a remarkably enhanced photoactivity was resulted, in comparison with pure  $\text{TiO}_2$ . Interestingly, when treated with mixture of organic dyes (RhB) and heavy metal ions, mesoporous titanium phosphonates showed an even higher activity for the degradation of organic dyes.<sup>82</sup> This could be the complex of metal ions on the surface of the hybrid network, resulting in a new broad absorption peak emerging in visible light region. This could thus give rise to a better use of visible light. While the presence of RhB did not prohibit the adsorption process of the heavy metal ions, it can be concluded that the hybrid phosphonate material could be used as an efficient and low-cost

catalyst and adsorbent for a one-pot wastewater cleanup with a large industrial potential.

Mesoporous phosphonated titania hybrid materials were prepared with the use of ATMP as the coupling molecule and triblock copolymer F127 as the template,<sup>115</sup> in which the phosphonate groups homogeneously anchored on the mesoporous titania, allowing monolayer adsorption of  $\text{Zn}^{2+}$  by extensive coordination with the organic bridging groups. The highly dispersed photoactive ZnO nanoparticles were then formed through low-temperature annealing (180 °C) of the  $\text{Zn}^{2+}$  adsorbed mesoporous phosphonated titania, and the resultant ZnO coupled mesoporous phosphonated titanium oxide photocatalysts exhibited excellent photocatalytic activity and stability in photo-degradation of Rhodamine B under both UV and visible light irradiation.<sup>148</sup> In comparison with the pristine mesoporous phosphonate titania, the commercial titania P25, and the ZnO/mesoporous titania prepared by the conventional impregnation, the superior photocatalytic performance and stability of the coupled catalyst of ZnO nanoparticles highly dispersed on the mesoporous phosphonated titania might be due to the coupling effect, the well-defined mesoporosity and the incorporation of phosphonic moieties into the  $\text{TiO}_2$  network, presenting the potential applications in the fields of environmental remediation and solar cells.

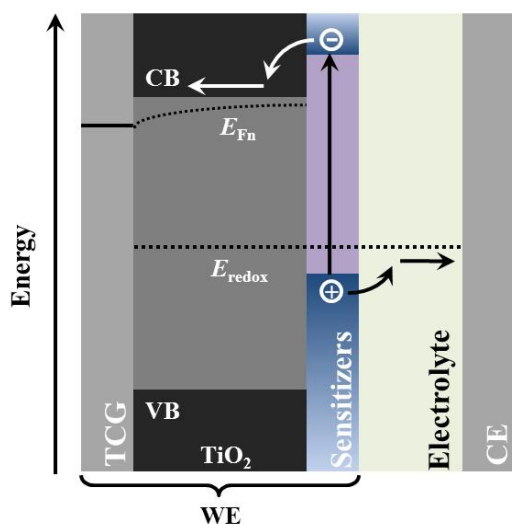


**Fig. 10** Schematic illustration of sensitized solar cells. A typical work electrode (WE) is composed of transparent conductive glass (TCG),  $\text{TiO}_2$  and sensitizers (organic dyes and quantum dots). The sensitized nanostructures are immersed in redox electrolyte, and the circuit is closed by a counter electrode (CE). The latter is usually illuminated through a counter electrode (CE). Energy-band diagram showing the conduction- (CB) and valence-band (VB) edges of the wide-bandgap semiconductor (e.g.,  $\text{TiO}_2$ ), the ground and excited level of the sensitizers and the redox potential  $E_{\text{redox}}$ . Upon solar light illumination, electrons are injected from the excited state into the  $\text{TiO}_2$ , while the oxidized QD is recharged by the redox electrolyte.

Solar sensitized cells (SSCs) have been intensively investigated since 1991.<sup>149,150</sup> Typical SSCs are consisted of three parts: work electrodes, counter electrodes, and liquid or polymeric electrolytes (Fig. 10). As to a work electrode,  $\text{TiO}_2$  is the commonly used semiconductor, performing as an electron

selective layer between the photo-sensitizers (organic dyes and quantum dots) and electron-collecting conducting glasses. Important aspects for optimization of the cell performance are selection of the photo-sensitizers and its attachment motif to the semiconductor surface. A number of dyes for most efficient dye-sensitized SSs (DSSCs) are ruthenium-polypyridyl complexes.<sup>151,152</sup> Though efficient in terms of good interfacial electronic coupling in DSSCs, dyes bearing carboxylate anchors have shown to be of limited stability in aqueous and highly oxidizing conditions,<sup>153</sup> and bifunctional long-chain carboxylic acids tend to form undesirable looping structures. Very recently, phosphonic acids were found to offer a promising alternative owing to their high affinity toward the surfaces of metal oxides and the relatively stronger bindings than carboxylic acids,<sup>154,155</sup> and they would thereby give better long-term stability of DSSCs. Mulhern *et al.* have analyzed the influence of the surface-attachment functions of the dyes on electron transfer at dye- $\text{TiO}_2$  interface and long-term stability.<sup>153</sup> Chalcogenorhodamine dyes were attached to the surface of nanocrystalline  $\text{TiO}_2$  through phosphonic or carboxylic acid functions. It was found that no significant changes in the photoelectrochemical performances of DSSCs. H aggregation (*i.e.* plane-to-plane  $\pi$ -stacking, which broadens the absorbance and causes a blue shift) and electron transfer reactivity were observed when varying the nature of the anchoring group. However, phosphonic linkers were found to enhance the dye- $\text{TiO}_2$  bonds stability, particularly upon immersion of the material in acidified acetonitrile. Obviously, carboxylic-functionalized dyes desorbed completely from  $\text{TiO}_2$  within 30 min, while only no more than 20% of desorption occurred with phosphonic-functionalized dyes after 2 days of immersion under the same conditions. By varying the solvent, pH, electrolyte, semiconductor, and presence of oxygen, Hanson *et al.* carried out a series of investigations of the relative desorption of  $-\text{PO}_3\text{H}_2$  versus  $-\text{COOH}$  substituted  $[\text{Ru}^{\text{II}}(\text{bpy})_3]^{2+}$  under different conditions.<sup>153</sup> Carboxylic-based dyes were found to detach between 5 and 1000 times faster than that of phosphonic counterparts in all tested media.

Nonetheless, in addition to the fact that phosphonic acids present more stable alternatives, the charge-injection rates can be prohibited to some extent due to the tetrahedral phosphorus center and loss of conjugation.<sup>156,157</sup> To combine the superiority of the binding stability of phosphonate and the good electron injection efficiency of carboxylate has testified to a feasible method (Fig. 11).<sup>158</sup> A bis(tridentate)-ruthenium complex containing phosphonic and carboxylic acids was elaborated.<sup>157</sup> The underlying basis of this strategy was that the carboxylate moiety needed only to be positioned on the ligand that was involved in charge transfer to the  $\text{TiO}_2$ , while the phosphonate moieties could be installed on the opposing ligand that did not need to participate directly in the injection process. This led to combine interesting electron injection properties from the dye into the semiconductor, and a good stability in aqueous media.

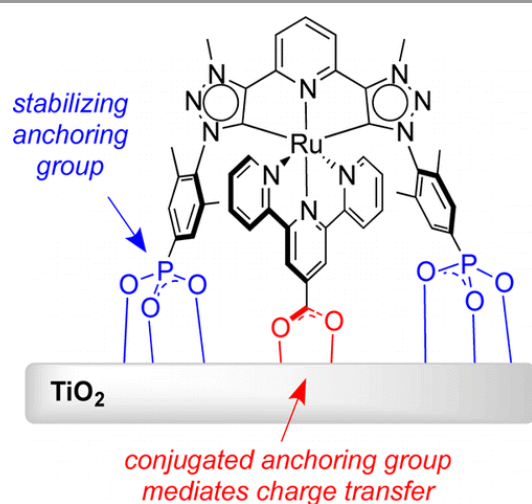


**Fig. 11** Ruthenium dye functionalized by both phosphonic and carboxylic acids were anchor on  $\text{TiO}_2$  substrate.<sup>158</sup>

The conventional preparation for the dye-sensitized electrodes of solar cells is accomplished by the adsorption of dye molecules onto the pre-synthesized semiconductor membranes, which usually leads to a very low loading amount of the photosensitive molecules.<sup>149,150,153</sup> The over-increasing of the loading amount would result in the dye aggregation. This actually is a waste of the high-cost dyes, because the poor contact between the aggregated dye molecules and the semiconductor could block the transmission of photoelectrons. Sol-gel method allows the molecular-level penetration of large  $\pi$ -aromatic photosensitive groups into the mesoporous semiconductor network homogeneously,<sup>159</sup> leading the achievement of an unprecedented high loading amount of organic dyes. Meanwhile, the aggregation of dye molecules could be efficiently suppressed. Thus the resultant mesoporous hybrids were proved to be efficient photocurrent conductors and better electrode materials than the traditional dye-modified titania materials under the same experimental conditions.<sup>159</sup> This model supplies us with an alternative strategy for the construction of new dye-sensitized solar cells from organic-inorganic hybrid mesoporous materials.

In the context of solar energy conversion, quantum-dot-sensitized solar cells (QDSSCs) are a promising alternative to existing photovoltaic technologies due to the tunable band gap and promise of stable, low-cost performance.<sup>160</sup> In addition, the QDs open up a way to utilize hot electrons and to generate multiple electron-hole pairs with a single photon through impact ionization. The use of organic linkers between the QDs and titania could provide a means of eliminating recombination and lead to the increased conversion efficiency and improved stability.<sup>160,161</sup> Ardalan *et al.* investigated the effects of self-assembled monolayers with phosphonic acid headgroups on the bonding and the performance of cadmium sulfide (CdS) SSCs.<sup>162</sup> Several organophosphonic acids with different tail-groups ( $-\text{NH}_2$ ,  $-\text{COOH}$  and  $-\text{CH}_3$ ) were taken as the linkers. It was demonstrated that the nature of the tail-group does not

significantly affect the uptake of CdS quantum dots on  $\text{TiO}_2$  nanocrystallites nor their optical properties, but the presence of the phosphonic-based linkers had a significant effect on the photovoltaic device performance. The power conversion efficiencies in devices made with phosphonic acids were up to  $\sim 3$  times higher than those without any anchoring agent, which might be due to that the organic linkers acted as recombination barriers or the passivated defects at the  $\text{TiO}_2$  surface.<sup>162</sup> Furthermore, the electron injection yield depends on the distance between QDs and  $\text{TiO}_2$ , and it decreases with the increase of linkage chain length.<sup>163,164</sup> This is a non-ignorable item in understanding functionality of phosphonic linkers and rational design of better photoelectrochemical materials.

Sensitized solar cells represent an indispensable role in sustainable development and the exploration of clean energy. It is noteworthy that phosphonate-based DSSCs and QDSSCs show inadequate photo-light conversion efficiency, though the corresponding stability of electrodes show potential in long term use. Since QDs can effectively capture solar energy due to the size-dependent adsorbance, QD-dye co-sensitized solar cells can be worthy of investigation. This not only can make full use of sun light, but also combines the peculiarities of QDs and organic dyes.

### 6.3.2 Proton conductivity for fuel cell applications

Extensive research has been devoted to realizing polymer-supported electrolyte membrane fuel cells consisting of perfluorosulfonic acid polymers (*e.g.*, Nafion); however, these polymers have some drawbacks, such as operation temperature, humidity, and cost.<sup>165</sup> The use of metal phosphonates as inexpensive proton-conducting membranes for fuel cell applications represents a rising research direction.<sup>13,30</sup> The phosphonate groups with three oxygen atoms can coordinate with metal ions into multidimensional hybrid frameworks, while the oxygen atoms may still be available to further perform as hydrogen-bonding acceptors.<sup>32</sup> These sites could serve to anchor carrier molecules or directly transfer protons as part of a conduction pathway. Taylor *et al.* reported the PCMOF3 with a layer structure,  $\text{Zn}_3(\text{L})(\text{H}_2\text{O})_2 \cdot 2\text{H}_2\text{O}$  ( $\text{L} = [1,3,5\text{-benzenetriphosphonate}]^{6-}$ ), in which the phosphonate and  $\text{Zn}^{2+}$  ions did not saturate each other's coordination spheres.<sup>166</sup> Thus the interlayer region was abundant in phosphonate oxygen atoms and Zn ligated water molecules. The resultant proton conductivity in  $\text{H}_2$  was measured as  $3.5 \times 10^{-5} \text{ S cm}^{-1}$  at 25 °C and 98% relative humidity (RH). An Arrhenius plot gave a low activation energy of 0.17 eV for proton transfer, indicating the Grotthuss hopping mechanism.<sup>166</sup>

Conductivity is a product of the magnitude of the charge, the number of charge carriers, and the mobility of the charges. Conductivity can be tuned by introducing the acidic and hydrophilic units, such as carboxylate, phosphonate and sulfonate groups, due to the presence of hydrophilic oxygen atoms to act as hydrogen-bonding acceptors. After the  $C_3$ -symmetric trisulfonate ligand in PCMOF2 (trisodium 2,4,6-trihydroxy-1,3,5-trisulfonate benzene) was isomorphously substituted with the  $C_3$ -symmetric tris(hydrogen phosphonate)

ligand, the resulting material PCMOF2<sup>1/2</sup> had its proton conduction raised 1.5 orders of magnitude compared to the parent material, to  $2.1 \times 10^{-2} \text{ S cm}^{-1}$  at 90% RH and 85 °C, while maintaining the parent MOF structure.<sup>167</sup> This was due to that the pores were partially lined with the hydrogen phosphonate groups rather than exclusively nonprotonated sulfonate groups, which should augment proton conduction. A series of MOF-polymer composite membranes exhibited the enhanced low-humidity proton conductivity, compared with that of pure MOF submicrometer crystals,  $\{[\text{Ca}(\text{D-Hmpc})(\text{H}_2\text{O})_2] \cdot 2\text{HO}_{0.5}\}_n$ , at 25 °C and ~ 53% RH.<sup>168</sup> It was found that the available proton carriers in the MOF structure provided a basis for the conductivity, and the large humidification effect of PVP with adsorbed water molecules greatly contributed to the proton transport in the composite membrane.

Phosphonate-based MOFs have gradually attracted scientists' interest. As discussed above, the efficient preparation of porous crystalline metal phosphonates is still confronted with many difficulties. If metal phosphonates are to serve as proton conductors for practical application, they were preferable function under relatively mild conditions (*e.g.*, at low temperatures and in anhydrous conditions). It is considered that this goal may be achieved through pre-protection or post-functionalization of the phosphonic bridging groups.

Notably, the considerable ion-exchange capability of metal phosphonates has been confirmed.<sup>133,134</sup> Zirconium tetraphosphonates possessed an open framework structure with 1D cavities decorated with polar and acids P=O and P-OH groups.<sup>169</sup> In addition to the excellent proton conductivity, the hybrid could be fully protonated by adding HCl and then subjected to several acid-base ion-exchange reactions with alkaline metal ions, such as Li<sup>+</sup>, Na<sup>+</sup>, and K<sup>+</sup>. Anionic MOF of  $\text{Zn}_{2.5}(\text{H})_{0.4-0.5}(\text{C}_6\text{H}_3\text{O}_9\text{P}_3)(\text{H}_2\text{O})_{1.9-2}(\text{NH}_4)_{0.5-0.6}$  was synthesized with the use of urea and 1,3,5-benzenetriphosphonic acid,<sup>170</sup> in which ammonium ions are exchangeable with Li<sup>+</sup>. Due to the certain degree of flexibility of the hybrid framework,<sup>13,32,34,170</sup> it can be envisioned the reversible insertion/desertion of Li<sup>+</sup> through the pores and elastic network, showing potential in secondary batteries. Although this aspect is not extensively studied, the intrinsic porosity within the conductive hybrid materials (ions or protons) remain largely unknown but is worthy of research efforts.

#### 6.4 Bioapplications

The capacity of metal phosphonates to be designed with specialized functionalities makes them promise great potential to be a new category of materials for bioapplications. Immobilization of enzymes on the proper solid supports can improve enzyme stability, facilitate separation and recycling, and maintain the catalytic activity and selectivity.<sup>171</sup> Mesoporous zirconium organophosphonates using 1-phosphomethylproline (H<sub>3</sub>PMP) as the bridging molecule possessed tunable mesopores, high surface area and large pore volume, exhibiting high adsorption capacity and adsorption rate for the enzyme.<sup>172</sup> For lysozyme (Lz) adsorption, the adsorption

equilibrium could be reached within 30 min. The adsorption capacity for Lz and papain reached as high as 438 and 297 mg g<sup>-1</sup>, respectively. Furthermore, Lz loaded on mesoporous zirconium phosphonates retained a structural conformation similar to that of its free state, suggesting that no denaturalization of Lz occurred during the adsorption process.<sup>163</sup> No leaching of Lz from the solid was observed when shaking the Lz-loaded solid in a buffer solution. The loading of biomolecules into the porous phosphonate hybrid networks is directly correlated with the strength of host-guest interactions,<sup>108</sup> surface area and pore size.<sup>171,172</sup> Correspondingly, separation of biomolecules can be feasibly realized through utilizing the targeted phosphonic bridging groups and adjusting the porosity of the phosphonate materials.

The incorporation of 1,4-bis(phosphomethyl)piperazine (BPMP) could introduce pH-sensitivity into the metal phosphonate hybrid networks.<sup>173</sup> The pH-sensitivity was derived from the reversible protonation under acidic conditions and deprotonation under weakly basic medium of piperazine moieties under different pH conditions, thereby endowing mesoporous zirconium phosphonates with reversible cationic-neutral surface properties. The designed delivery systems of "molecular lock" are able to selectively release the entrapped guests. For instance, the negatively charged PDS (a photosensitizer of sulfonated phthalocyanine for photodynamic therapy of tumors) could then be adsorbed or released through strong electrostatic interaction according to the pH condition. The integration of H<sub>3</sub>PMP and BPMP would lead to the phosphonate hybrids with bifunctionality, pH-sensitivity and functionalizability.<sup>174</sup> The reversible protonation-deprotonation of L-proline groups of H<sub>3</sub>PMP and piperazine groups of BPMP on the mesoporous walls under different pH values (pH sensitivity) as well as the further functionalization with cell-penetrating peptides *via* the carboxyl in L-proline group of H<sub>3</sub>PMP on outer surface (functionalizability) endowed the materials with pH-controllable release function and high cell penetration capability, respectively.<sup>174</sup> Thus a time- and pH-controlled oral colon-targeted nucleic acid delivery system was developed. Using salmon sperm DNA as model nucleic acid, it could remain intact during delivery. The penetration capability through biomembranes could be enhanced through further functionalization with a cell-penetrating peptide of octarginine.

Numerous studies have indicated that nanoparticle-based therapeutics and diagnostic agents show enhanced efficacy and reduced side effects, due to their unique physicochemical properties.<sup>175,176</sup> The vast majority of nanocarriers can be classified into two categories: either purely inorganic (*e.g.*, quantum dots) or purely organic (*e.g.*, liposomes). Noticeably, nanosized metal phosphonate hybrids have the potential to combine attractive characteristics of both inorganic and organic nanocarriers including robust particle morphologies, compositional and structural diversity, biocompatibility and bioactivity, to provide an unique platform for delivering agents, therapeutics and biosensing.<sup>23,31,177</sup> Surface-modification of iron oxide nanoparticles by phosphonates have a wealth of applications including magnetic resonance imaging (MRI), drug

delivery and hyperthermia for cancer treatment.<sup>178-180</sup> Lartigue *et al.* reported the modification of iron oxide nanoparticles with carbohydrates derivatized by phosphonate groups.<sup>180</sup> The magnetic, hyperthermal, and relaxometric properties of the phosphonated nanoparticles made them promising for MRI imaging and hyperthermia. On the basis of poly(quaternary ammonium) brushes grown by atom transfer radical polymerization using an initiator grafted via a phosphonate group to the surface of magnetite nanoparticles,<sup>181</sup> recyclable antibacterial magnetic nanoparticles were successfully synthesized. Since the convenience to separate from the bacterial culture tests using an external magnetic field, the resultant nanoparticles presented a high biocidal activity against *E. coli* bacteria even after eight exposure tests. When cyclodextrin groups were attached to magnetite nanoparticles by using a phosphonic linkage,<sup>182</sup> the anchored cyclodextrin formed inclusion complexes with Diclofenac sodium salt, a non-steroidal anti-inflammatory drug, demonstrating the potential for targeted drug delivery.

In the past few years, some implant semiconductor biomaterials functionalized by phosphonic acids, such as  $\text{In}_2\text{O}_3$  and  $\text{TiO}_2$ , have been investigated for biosensor applications.  $\text{In}_2\text{O}_3$  nanowires were first grafted with 3-phosphonopropionic acid, and then the terminal carboxylic acid groups were activated by EDC/NHS aqueous solution,<sup>183</sup> resulting in a nanowire surface reactive toward the amine groups present on antibodies. After passivation with an amphiphathic polymer (Tween 20), the resultant sensors were found to be capable of performing rapid, label-free, electrical detection of cancer biomarkers directly from human whole blood collected by a finger prick. However, up to now, detection and medication of organism diseases are two consecutive and inseparable processes in clinical diagnostics and treatment, but their academic studies are often isolated from each other. It is still challenging and significant to design a “diagnospy” carrier that combines the functions of biomolecule quantitative detection and bioresponsive drug controlled release.<sup>184,185</sup> Li *et al.* pioneered a study to intentionally design a smart system on the basis of hybrid phosphonate- $\text{TiO}_2$  mesoporous nanostructures capped with fluorescein labelled oligonucleotides, which could realize simultaneous and highly-efficient biomolecule sensing and controlled drug release (Fig. 12).<sup>186</sup> The incorporation of phosphonate could shift the absorption edge of titania to visible light range and introduce positively charged amino groups to interact with negatively charged fluorescein labelled oligonucleotides, resulting in the closing of the mesopores and the fluorescence quenching of fluorescein at the same time. The further addition of complementary single DNA strands or protein target led to the displacement of the capped DNA due to hybridization or protein-aptamer reactions. Correspondingly, the pores were opened, causing the release of entrapped drugs as well as the restoration of dye fluorescence. Moreover, target concentration-dependent fluorescence signal response could be used to real-time monitor treatment effects, thus providing proof for determining drug dose or adjusting the treatment program. This provides a novel perception to utilize non-

siliceous hybrid materials as the supports in sensing and control release applications.

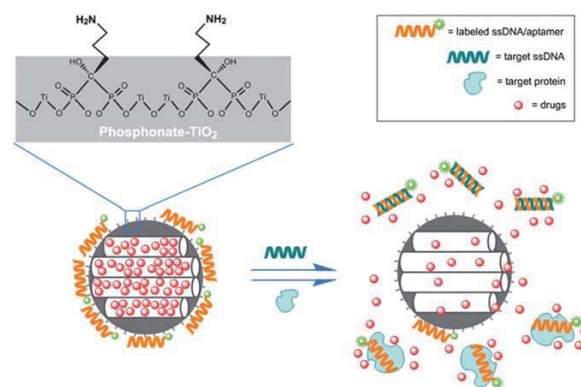


**Fig. 12** Schematic illustration of bioresponsive detection and drug controlled release system based on phosphonate- $\text{TiO}_2$  hybrid material.<sup>186</sup>

Metal phosphonates are latent host materials in the fields of biosensing and biotechnology owing to the well-defined porosity, low biotoxicity and capacity of incorporation of biogroups. Introduction of specific organophosphonic linkers could result in biomimic performance. However, many practical detecting or sensing applications require extraordinarily high sensitivities. Optical sensors are molecular receptors whose optical properties can be changed upon binding to specific guests. Optical sensing and imaging systems have been intensively investigated for their capability of providing high sensitivity, fast and easy detection processing, biocompatibility, and adaptability to a wide variety of conditions.<sup>187</sup> Since lanthanide phosphonates are photoluminescent hybrid materials with ease of functionalization,<sup>50-54</sup> they are a promising class of materials for applications in sensing and optical imaging.<sup>177,188</sup> These areas are of great significance to be explored.

## 7 Summary and outlook

Inorganic-organic metal phosphonate materials and the related hybrid nanocomposites have received tremendous attention in the past decades due to the unique physicochemical properties. Due to the less predictable coordination chemistry of phosphonate linkers, densely structured phosphonate motifs are formed. Through inserting non-pillaring spacers, complicating the organophosphonic linkages and attaching a functional group on the ligand could lead to the creation of porosity in the hybrid frameworks. To improve the accessibility of the porous systems, template-free and surfactant-assisted strategies on the basis of sol-gel chemistry have proven to be effective in obtaining porous phosphonate hybrids with adjustable porosity. Surface modification of the inorganic oxide substrates with phosphonates can not only preserve the nature of bulk, but also control the surface and interface properties of materials. The developments in modification of metal phosphonates demonstrate how modern physical techniques and chemical design can be applied to functionalize their internal

surfaces. Metal phosphonate hybrid and the relevant composites have demonstrated significant potential ranging from adsorption/separation and catalysis to the burgeoning biotechnology and energy conversion and storage.

Although metal phosphonates have shown to outperform other porous materials in some applications, the relatively inferior stability of the hybrid materials compared with inorganic frameworks has impeded the further application potential. The effort for the enhancement of the thermal and hydrothermal stability of the metal phosphonate materials should be of great attention, and the crystalline pore wall is the most expected. However, for phosphonates, the unpredictable ligating mode would facilitate the formation of networks, on the contrary, it could result in precipitates with low degrees of order. Furthermore, it remains contradictory and challenging to achieve the high crystallization and well-structured hierarchical porosity (especially micro-/mesoporosity) simultaneously. The coordination rate between the inorganic units and organic moieties determines the nucleation kinetics and thus the crystal growth.<sup>189</sup> "Crown-mediated controlled-release" methodology has recently exhibited the availability in constructing porous sulfonate- and carboxylate-based MOFs,<sup>189,190</sup> which might provide a new route in rational designing crystalline metal phosphonate with well-defined porous structures. Considering the intimate relations between phosphonates and phosphates, phosphonates may act as precursors in preparing phosphates with interesting structures and novel properties, thus improving the performances of phosphates in catalysis, photoelectricity and secondary batteries.<sup>191-194</sup>

Overall, the development in inorganic-organic metal phosphonate materials signifies a pivotal step towards exploring and finding new multifunctional hybrid materials and has significantly expanded the applicable application ranges. Nowadays, the molecular approaches of solid state chemistry and organic synthesis chemistry have reached a high level of sophistication. As a consequence, original phosphonate hybrids can be designed through the synthesis of new hybrid nanosynths, allowing for the coding of hybrid assemblies presenting a spatial ordering at different length scales. Particularly, the synthesis through the simultaneous use of self-assembly process together with external factors, such as electrical or magnetic fields, or even through the use of strong compositional flux variations of the reagents during the synthesis are worthwhile to explore. The increasing interest of the field of functional hybrid metal phosphonate materials will be amplified in the future by the growing interest of materials scientists, chemists and biologists to fully exploit this opportunity for discovering materials and devices benefiting from the best of the two realms: inorganic and organic.

## Acknowledgement

This work was supported by the National Natural Science Foundation of China (21076056 and 21073099), the Specialized Research Fund for the Doctoral Program of Higher Education (20110031110016), the Program for Innovative

Research Team in University (IRT13022), and the 111 project (B12015). Z.Y.Y. also thanks to the support from the Royal Academy of Engineering for a Research Exchanges with China and India Award.

## Notes and references

<sup>a</sup> Key Laboratory of Advanced Energy Materials Chemistry (Ministry of Education), Collaborative Innovation Center of Chemical Science and Engineering (Tianjin), College of Chemistry, Nankai University, Tianjin 300071, China. E-mail: [zyyuan@nankai.edu.cn](mailto:zyyuan@nankai.edu.cn).

<sup>b</sup> School of Chemical Engineering and Technology, Hebei University of Technology, Tianjin 300130, China.

- 1 J. Livage and J. Lemerle, *Annu. Rev. Mater. Sci.*, 1982, **12**, 103.
- 2 J. Livage, *Chem. Mater.*, 1991, **3**, 578.
- 3 J. Livage, M. Henry and C. Sanchez, *Prog. Solid State Chem.*, 1988, **18**, 259.
- 4 J. Livage, *New J. Chem.*, 2001, **25**, 1.
- 5 C. Sanchez and J. Livage, *New J. Chem.*, 1990, **14**, 503.
- 6 K. Nakanishi and K. Kanamori, *J. Mater. Chem.*, 2005, **15**, 3776.
- 7 P. Innocenzia and B. Lebeau, *J. Mater. Chem.*, 2005, **15**, 3821.
- 8 W. J. Hunks and G. A. Ozin, *J. Mater. Chem.*, 2005, **15**, 3716.
- 9 S. Mann, *Biomimetic Materials Chemistry*, Wiley-VCH, Weinheim, 1997.
- 10 S. Mann, *Angew. Chem., Int. Ed.*, 2000, **39**, 3393.
- 11 P. Gomez-Romero, *Adv. Mater.*, 2001, **13**, 163.
- 12 R. Gangopadhyay and A. De, *Chem. Mater.*, 2000, **12**, 608.
- 13 G. K. H. Shimizu, R. Vaidhyanathan and J. M. Taylor, *Chem. Soc. Rev.*, 2009, **38**, 1430.
- 14 C. Sanchez and F. Ribot, *New J. Chem.*, 1994, **18**, 1007.
- 15 P. Judeinstein and C. Sanchez, *J. Mater. Chem.*, 1996, **6**, 511.
- 16 R. J. P. Corriu, *New J. Chem.*, 2001, **25**, 2.
- 17 T. Z. Ren, Z. Y. Yuan, L. B. Su, *Chem. Chommun.*, 2004, 2730.
- 18 E.G. Vrieling, T.P.M. Beelen, R.A. van Santen and W. W. C. Gieskes, *Angew. Chem. Int. Ed.*, 2002, **41**, 1543.
- 19 C. Sanchez, L. Rozes, F. Ribot, C. Laberty-Robert, D. Grosso, C. Sassoie, C. Boissiere and L. Nicole, *C. R. Chimie*, 2010, **13**, 3.
- 20 S. Inagaki, S. Guan, Y. Fukushima, T. Ohsuna and O. Terasaki, *J. Am. Chem. Soc.*, 1999, **121**, 9611.
- 21 T. Asefa, M. J. MacLachlan, N. Coombs and G. A. Ozin, *Nature*, 1999, **402**, 867.
- 22 B. J. Melde, B. T. Holland, C. F. Blanford and A. Stein, *Chem. Mater.*, 1999, **11**, 3302.
- 23 Y. P. Zhu, T. Z. Ren and Z. Y. Yuan, *New J. Chem.*, 2014, DOI: 10.1039/C3NJ01139A.
- 24 A. Clearfield and Z. Wang, *J. Chem. Soc., Dalton Trans.*, 2002, **15**, 2937.
- 25 A. Clearfield, *Curr. Opin. Solid State Mater. Sci.*, 1996, **1**, 268.
- 26 M. E. Davis, *Nature*, 2002, **417**, 813.
- 27 M. Eddaoudi, J. Kim, N. Rosi, D. Vodak, J. Wachter, M. O'Keeffe and O. M. Yaghi, *Science*, 2002, **295**, 469.
- 28 K. S. W. Sing, D. H. Everett, R. H. W. Haul, L. Moscou, R. A. Pierotti, J. Rouquerol and T. Siemieniewska, *Pure Appl. Chem.*, 1985, **57**, 603.
- 29 T. Kimura, *J. Nanosci. Nanotechnol.*, 2013, **13**, 2461.
- 30 A. Clearfield, *Dalton Trans.*, 2008, 6089.

- 31 T. Y. Ma and Z. Y. Yuan, *ChemSusChem*, 2011, **4**, 1407.
- 32 K. J. Gagnon, H. P. Perry and A. Clearfield, *Chem. Rev.*, 2012, **112**, 1034.
- 33 K. Maeda, *Micropor. Mesopor. Mater.*, 2004, **73**, 47.
- 34 A. Clearfield, C. V. K. Sharma and B. L. Zhang, *Chem. Mater.*, 2001, **13**, 3099.
- 35 R. C. Finn, R. Lam, J. E. Greedan and J. Zubieta, *Inorg. Chem.*, 2001, **40**, 3745.
- 36 C. Herdes, A. Valente, Z. Lin, J. Rocha, A. A. P. Coutinho, F. Medina and L. F. Vega, *Langmuir*, 2007, **23**, 7299.
- 37 D. B. Mitzi, *Chem. Mater.*, 2001, **13**, 3283.
- 38 F. Fredoueil, M. Evain, D. Massiot, M. Bujoli-Doeuff and B. Bujoli, *J. Mater. Chem.*, 2001, **11**, 1106.
- 39 J. L. Snover, H. Byrd, E. P. Suponeva, E. Vicenzi and M. E. Thompson, *Chem. Mater.*, 1996, **8**, 1490.
- 40 G. Alberti, U. Costantino, S. Allulli and N. Tomssini, *Inorg. Nud. Chem.*, 1978, **4**, 1113.
- 41 G. Y. Yang and A. Clewfield, *Raacr. Pofym.*, 1987, **5**, 13.
- 42 C. Y. Ortiz-Avila and A. Clewfield, *Inorg. Chem.*, 1985, **24**, 1773.
- 43 H. Byrd, A. Clearfield, D. Poojary, K. P. Reis and M. E. Thompson, *Chem. Mater.*, 1996, **8**, 2239.
- 44 A. Clearfield, Z. K. Wang and P. Bellinghausen, *J. Solid State Chem.*, 2002, **167**, 376.
- 45 J. G. Mao, *Coordin. Chem. Rev.*, 2007, **251**, 1493.
- 46 O. R. Evans, H. L. Ngo and W. B. Lin, *J. Am. Chem. Soc.*, 2001, **123**, 10395.
- 47 H. L. Ngo and W. B. Lin, *J. Am. Chem. Soc.*, 2002, **124**, 14298.
- 48 A. Clearfield, C. V. K. Sharma and B. L. Zhang, *Chem. Mater.*, 2001, **13**, 3099.
- 49 S. W. A. Bligh, N. Choi, C. F. G. C. Gerald, S. Knoke, M. McPartlin, M. J. Sangane and T. M. Woodroffe, *J. Chem. Soc., Dalton Trans.*, 1997, 4119.
- 50 F. N. Shi, L. Cunha-Silva, R. A. S. Ferreira, L. Mafra, T. Trindade, L. D. Carlos, F. A. A. Paz and J. Rocha, *J. Am. Chem. Soc.*, 2008, **130**, 150.
- 51 L. Cunha-Silva, L. Mafra, D. Ananias, L. D. Carlos, J. Rocha and F. A. A. Paz, *Chem. Mater.*, 2007, **19**, 3527.
- 52 S. M. Ying and J. G. Mao, *Cryst. Growth Des.*, 2006, **6**, 964.
- 53 B. P. Yang, A. V. Prosvirin, Y. Q. Guo and J. G. Mao, *Inorg. Chem.*, 2008, **47**, 1453.
- 54 P. Rabu, P. Janvier and B. Bujoli, *J. Mater. Chem.*, 1999, **9**, 1323.
- 55 J. G. Mao, Z. K. Wang and A. Clearfield, *Inorg. Chem.*, 2002, **41**, 6106.
- 56 J. T. Li, L. R. Guo, Y. Shen and L. M. Zheng, *CrystEngComm*, 2009, **11**, 1674.
- 57 J. Bideau, C. Le, Payen, P. Palvadeau and B. Bujoli, *Inorg. Chem.*, 1994, **33**, 4885.
- 58 K. Maeda, Y. Kiyozumi and F. Mizukami, *Angew. Chem., Int. Ed.*, 1994, **33**, 2335.
- 59 K. Maeda, J. Akimoto, Y. Kiyozumi and F. Mizukami, *Angew. Chem., Int. Ed.*, 1995, **34**, 1199.
- 60 D. L. Lohse and S. C. Sevov, *Angew. Chem., Int. Ed.*, 1997, **36**, 1619.
- 61 R. N. Devi, P. Wormald, P. A. Cox and P. A. Wright, *Chem. Mater.*, 2004, **16**, 2229.
- 62 E. V. Bakmutova, X. Ouyang, D. G. Medvedev and A. Clearfield, *Inorg. Chem.*, 2003, **42**, 7046.
- 63 L. M. Zheng, H. H. Song, C. Y. Duan and X. Q. Xin, *Inorg. Chem.*, 1999, **38**, 5061.
- 64 A. Turner, B. P. A. Jaffres, E. J. MacLean, D. Villemin, V. McKee and G. B. Hix, *Dalton Trans.*, 2003, **7**, 1314.
- 65 G. Guerrero, J. G. Alauzun, M. Granier, D. Laurencin and P. H. Mutin, *Dalton Trans.*, 2013, **42**, 12569.
- 66 H. P. Perry, J. Law, J. Zon and A. Clearfield, *Micropor. Mesopor. Mater.*, 2012, **149**, 172.
- 67 C. Serre, N. Stock, T. Bein and G. Férey, *Inorg. Chem.*, 2004, **43**, 3159.
- 68 Q. Yue, J. Yang, G. H. Li, G. D. Li and J. S. Chen, *Inorg. Chem.*, 2006, **45**, 4431.
- 69 M. Vasylyev and R. Neumann, *Chem. Mater.*, 2006, **18**, 2781.
- 70 M. Vasylyev, E. J. Wachtel, R. Popovitz-Biro and R. Neumann, *Chem. Eur. J.*, 2006, **12**, 3507.
- 71 L. Nicole, C. Boissière, D. Grosso, A. Quach and C. Sanchez, *J. Mater. Chem.*, 2005, **15**, 3598.
- 72 G. Alberti, F. Marmottini, R. Vivani and P. Zappelli, *J. Porous Mater.*, 1998, **5**, 221.
- 73 Y. P. Zhu, Y. L. Liu, T. Z. Ren and Z. Y. Yuan, Mesoporous nickel phosphate/phosphonate hybrid microspheres with excellent performance for adsorption and catalysis, *Submitted*.
- 74 C. T. Kresge, M. E. Leonowicz, W. J. Roth, J. C. Vartuli and J. S. Beck, *Nature*, 1992, **359**, 710–712.
- 75 N. Pal and A. Bhaumik, *Adv. Colloid Interf. Sci.*, 2013, **189**, 21.
- 76 T. Y. Ma, L. Liu and Z. Y. Yuan, *Chem. Soc. Rev.*, 2013, **42**, 3977.
- 77 J. El. Haskouri, C. Guillem, J. Latorre, A. Beltrán, D. Beltrán and P. Amorós, *Eur. J. Inorg. Chem.*, 2004, 1804.
- 78 J. El. Haskouri, C. Guillem, J. Latorre, A. Beltrán, D. Beltrán and P. Amorós, *Chem. Mater.*, 2004, **16**, 4359.
- 79 T. Kimura, *Chem. Mater.*, 2003, **15**, 3742.
- 80 T. Kimura, *Chem. Mater.*, 2005, **17**, 337.
- 81 T. Kimura, *Chem. Mater.*, 2005, **17**, 5521.
- 82 T. Y. Ma, X. Z. Lin and Z. Y. Yuan, *J. Mater. Chem.*, 2010, **20**, 7406.
- 83 T. Kimura, D. Nakashima and N. Miyamoto, *Chem. Lett.*, 2009, **38**, 916.
- 84 Y. H. Deng, J. Wei, Z. K. Sun and D. Y. Zhao, *Chem. Soc. Rev.*, 2013, **42**, 4054.
- 85 Y. Wan and D. Y. Zhao, *Chem. Rev.*, 2007, **107**, 2821.
- 86 T. Y. Ma, X. Z. Lin and Z. Y. Yuan, *Chem. Eur. J.*, 2010, **16**, 8487.
- 87 Q. S. Huo, D. I. Margolese and G. D. Stucky, *Chem. Mater.*, 1996, **8**, 1147.
- 88 T. Kimura and Y. Yamauchi, *Chem. Asian J.*, 2013, **8**, 160.
- 89 T. Kimura and Y. Yamauchi, *Langmuir*, 2012, **28**, 12901.
- 90 Z. Y. Yuan and B. L. Su, *J. Mater. Chem.*, 2006, **16**, 663.
- 91 T. Z. Ren, Z. Y. Yuan and B. L. Su, *Chem. Commun.*, 2004, 2730.
- 92 M. Pramanik and A. Bhaumik, *J. Mater. Chem. A*, 2013, **1**, 11210.
- 93 A. Dutta, A. K. Patra and A. Bhaumik, *Micropor. Mesopor. Mater.*, 2012, **155**, 208.
- 94 P. Yang, T. Deng, D. Zhao, P. Feng, D. Pine, B. F. Chmelka, G. M. Whitesides and G. D. Stucky, *Science*, 1998, **282**, 2244.
- 95 A. Imhof and D. J. Pine, *Nature*, 1997, **389**, 948.
- 96 K. J. Nakanishi, *J. Porous Mater.*, 1997, **4**, 67.
- 97 T. Amatani, K. Nakanishi, K. Hirao and T. Kodaira, *Chem. Mater.*, 2005, **17**, 2114.

- 98 T. Y. Ma, X. J. Zhang, G. S. Shao, J. L. Cao and Z. Y. Yuan, *J. Phys. Chem. C*, 2008, **112**, 3090.
- 99 X. Y. Yang, A. Leonard, A. Lemaire, G. Tian and B. L. Su, *Chem. Commun.*, 2011, **47**, 2763.
- 100 Z. Y. Yuan, T. Z. Ren, A. Azioune, J. J. Pireaux and B. L. Su, *Chem. Mater.*, 2006, **18**, 1753.
- 101 T. Y. Ma, X. J. Zhang and Z. Y. Yuan, *Micropor. Mesopor. Mater.*, 2009, **123**, 234.
- 102 X. J. Zhang, T. Y. Ma and Z. Y. Yuan, *Eur. J. Inorg. Chem.*, 2008, 2721.
- 103 T. Y. Ma and Z. Y. Yuan, *Eur. J. Inorg. Chem.*, 2010, **19**, 2941.
- 104 S. Polarz, B. Smarsly, L. Bronstein and M. Antonietti, *Angew. Chem. Int. Ed.*, 2001, **40**, 4417.
- 105 M. Bonini, S. Rossi, G. Karlsson, M. Almgren, P. L. Nostro and P. Baglioni, *Langmuir*, 2006, **22**, 1478.
- 106 T. Y. Ma, X. Z. Lin, X. J. Zhang and Z. Y. Yuan, *New J. Chem.*, 2010, **34**, 1209.
- 107 T. Y. Ma, X. Z. Lin, X. J. Zhang and Z. Y. Yuan, *Nanoscale*, 2011, **3**, 1690.
- 108 T. Y. Ma, X. J. Zhang and Z. Y. Yuan, *J. Phys. Chem. C*, 2009, **113**, 12854.
- 109 W. H. Deng and B. H. Shanks, *Chem. Mater.*, 2005, **17**, 3092.
- 110 H. Lee, L. J. Kepley, H. G. Hong and T. E. Mallouk, *J. Am. Chem. Soc.*, 1988, **110**, 618.
- 111 G. Guerrero, P. H. Mutin and A. Vioux, *Chem. Mater.*, 2001, **13**, 4367.
- 112 S. Marcinko and A. Y. Fadeev, *Langmuir*, 2004, **20**, 2270.
- 113 P. C. Angelomé and G. J. de A. A. Soler-Illia, *Chem. Mater.*, 2005, **17**, 3223.
- 114 P. C. Angelomé and G. J. de A. A. Soler-Illia, *J. Mater. Chem.*, 2005, **15**, 3903.
- 115 X. J. Zhang, T. Y. Ma and Z. Y. Yuan, *J. Mater. Chem.*, 2008, **18**, 2003.
- 116 T. Y. Ma, X. J. Zhang and Z. Y. Yuan, *J. Mater. Sci.*, 2009, **44**, 6775.
- 117 L. Liu, Q. F. Deng, X. X. Hou and Z. Y. Yuan, *J. Mater. Chem.*, 2012, **22**, 15540.
- 118 L. Liu, Q. F. Deng, T. Y. Ma, X. Z. Lin, X. X. Hou, Y. P. Liu and Z. Y. Yuan, *J. Mater. Chem.*, 2011, **21**, 16001.
- 119 R. Serna-Guerrero, E. Dána and A. Sayari, *Ind. Eng. Chem. Res.*, 2008, **47**, 9406.
- 120 Z. X. Wu, N. Hao, G. K. Xiao, L. Y. Liu, P. Webley and D. Y. Zhao, *Phys. Chem. Chem. Phys.*, 2011, **13**, 2495.
- 121 H. Furukawa, K. E. Cordova, M. O'Keeffe and O. M. Yaghi, *Science*, 2013, **341**, 974.
- 122 S. S. Iremonger, J. M. Liang, R. Vaidhyanathan, I. Martens, G. K. H. Shimizu, T. D. Daff, M. Z. Aghaji, S. Yeganegi and Tom K. Woo, *J. Am. Chem. Soc.*, 2011, **133**, 20048.
- 123 F. P. Zhai, Q. S. Zheng, Z. X. Chen, Y. Ling, X. F. Liu, L. H. Weng and Y. M. Zhou, *CrystEngComm*, 2013, **15**, 2040.
- 124 L. F. Song, J. Zhang, L. X. Sun, F. Xu, F. Li, H. Z. Zhang, X. L. Si, C. L. Jiao, Z. B. Li, S. Liu, Y. L. Liu, H. Y. Zhou, D. L. Sun, Y. Du, Z. Cao and Z. Gabelica, *Energy Environ. Sci.*, 2012, **5**, 7508.
- 125 G. P. Knowles, S. W. Delaney and A. L. Chaffee, *Ind. Eng. Chem. Res.*, 2006, **45**, 2626.
- 126 T.-Z. Ren, X.-H. Zhu, T.-Y. Ma, Z.-Y. Yuan, *Adsorpt. Sci. Technol.*, 2013, **31**, 535.
- 127 V. Lykourinou, Y. Chen, X. S. Wang, L. Meng, T. Hoang, L. J. Ming, R. L. Musselman and S. Q. Ma, *J. Am. Chem. Soc.*, 2011, **133**, 10382.
- 128 F. N. Shi, L. Cunha-Silva, R. A. S. Ferreira, L. Mafra, T. Trindade, L. D. Carlos, F. A. A. Paz and J. Rocha, *J. Am. Chem. Soc.*, 2008, **130**, 150.
- 129 T. Salesch, S. Bachmann, S. Brugger, R. Rabelo-Schaefer, K. Albert, S. Steinbrecher, E. Plies, A. Mehdi, C. Reyé, R. J. P. Corriu and E. Lindner, *Adv. Funct. Mater.*, 2002, **13**, 134.
- 130 T. Y. Ma, H. Li, A. N. Tang and Z. Y. Yuan, *Small*, 2011, **4**, 1407.
- 131 A. Dutta, A. K. Patra, H. Uyama and A. Bhaumik, *ACS Appl. Mater. Interf.*, 2013, **5**, 9913.
- 132 M. Pramanik and A. Bhaumik, *Chem. Eur. J.*, 2013, **19**, 8507.
- 133 X. Z. Lin and Z. Y. Yuan, *Eur. J. Inorg. Chem.*, 2012, 2661.
- 134 T. Y. Ma, L. Liu, Q. D. Deng, X. Z. Lin and Z. Y. Yuan, *Chem. Commun.*, 2011, **47**, 6015.
- 135 M. Pramanik, M. Nandi, H. Uyama and A. Bhaumik, *Catal. Sci. Technol.*, 2012, **2**, 613.
- 136 A. Dutta, M. Pramanik, A. K. Patra, M. Nandi, H. Uyama and A. Bhaumik, *Chem. Commun.*, 2012, **48**, 6738.
- 137 A. A. G. Shaikh and S. Sivaram, *Chem. Rev.*, 1996, **96**, 951.
- 138 J. L. Song, Z. F. Zhang, S. Q. Hu, T. B. Wu, T. Jiang and B. X. Han, *Green Chem.*, 2009, **11**, 1031.
- 139 D. A. Yang, H. Y. Cho, J. Kim, S. T. Yang and W. S. Ahn, *Energy Environ. Sci.*, 2012, **5**, 6465.
- 140 Y. W. Ren, Y. C. Shi, J. X. Chen, S. R. Yang, C. R. Qi and H. F. Jiang, *RSC Adv.*, 2013, **3**, 2167.
- 141 D. W. Feng, W. C. Chung, Z. W. Wei, Z. Y. Gu, H. L. Jiang, Y. P. Chen, D. J. Darensbourg and H. C. Zhou, *J. Am. Chem. Soc.*, 2013, **135**, 17105.
- 142 J. Kim, S. N. Kim, H. G. Jang, G. Seo and W. S. Ahn, *Appl. Catal. A*, 2013, **453**, 175.
- 143 T. Y. Ma and Z. Y. Yuan, *Chem. Commun.*, 2010, **46**, 2325.
- 144 T. Y. Ma and Z. Y. Yuan, *Dalton Trans.*, 2010, **39**, 9570.
- 145 J. L. Cao, Y. Wang, X. L. Yu, S. R. Wang, S. H. Wu and Z. Y. Yuan, *Appl. Catal. B*, 2008, **79**, 26.
- 146 H. P. Perry, J. Law, J. Zon and A. Clearfield, *Micropor. Mesopor. Mater.*, 2012, **149**, 172.
- 147 X. Y. Liu, A. Q. Wang, X. F. Yang, T. Zhang, C. Y. Mou, D. S. Su and J. Li, *Chem. Mater.*, 2009, **21**, 410.
- 148 Y. P. Zhu, T. Y. Ma, T. Z. Ren, J. Li, G. H. Du and Z. Y. Yuan, *Appl. Catal. B*, 2014, **156-157**, 44.
- 149 B. O'Regan and M. Grätzel, *Nature*, 1991, **353**, 737.
- 150 J. Burschka, N. Pellet, S. J. Moon, R. Humphry-Baker, P. Gao, M. K. Nazeeruddin and M. Grätzel, *Nature*, 2013, **499**, 316.
- 151 P. G. Bomben, K. C. D. Robson, B. D. Koivisto and C. P. Berlinguette, *Coord. Chem. Rev.*, 2012, **256**, 1438.
- 152 G. C. Vougioukalakis, A. I. Philippopoulos, T. Stergiopoulos and P. Falaras, *Coord. Chem. Rev.*, 2011, **255**, 2602.
- 153 K. Hanson, M. K. Brennaman, H. Luo, C. R. K. Glasson, J. J. Concepcion, W. Song and T. J. Meyer, *ACS Appl. Mater. Interf.*, 2012, **4**, 1462.
- 154 T. P. Brewster, S. J. Konezny, S. W. Sheehan, L. A. Martini, C. A. Schmuttenmaer, V. S. Batista and R. H. Crabtree, *Inorg. Chem.*, 2013, **52**, 6752.
- 155 R. Luschtinetz, J. Frenzel, T. Milek and G. Seifert, *J. Phys. Chem. C*, 2009, **113**, 5730.

- 156 K. R. Mulhern, A. Orchard, D. F. Watson and M. R. Detty, *Langmuir*, 2012, **28**, 7071.
- 157 K. Hanson, M. K. Brennaman, A. Ito, H. Luo, W. Song, K. A. Parker, R. Ghosh, M. R. Norris, C. R. K. Glasson, J. J. Concepcion, R. Lopez and T. J. Meyer, *J. Phys. Chem. C*, 2012, **116**, 14837.
- 158 D. G. Brown, P. A. Schauer, J. Borau-Garcia, B. R. Fancy and C. P. Berlinguette, *J. Am. Chem. Soc.*, 2013, **135**, 1692.
- 159 T. Y. Ma, Y. S. Wei, T. Z. Ren, L. Liu, Q. Guo and Z. Y. Yuan, *ACS Appl. Mater. Interfaces*, 2010, **2**, 3563.
- 160 S. Rühle, M. Shalom and A. Zaban, *ChemPhysChem*, 2010, **11**, 2290.
- 161 I. Robel, V. Subramanian, M. Kuno and P. V. Kamat, *J. Am. Chem. Soc.*, 2006, **128**, 2385.
- 162 P. Ardalan, T. P. Brennan, H. Lee, J. R. Bakke, I. K. Ding, M. D. McGehee and S. F. Bent, *ACS Nano*, 2011, **3**, 1495.
- 163 R. S. Dibbell, D. G. Youker and D. F. Watson, *J. Phys. Chem. C*, 2009, **113**, 18643.
- 164 R. S. Dibbell and D. F. Watson, *J. Phys. Chem. C*, 2009, **113**, 3139.
- 165 Q. Li, R. He, J. O. Jensen and N. J. Bjerrum, *Chem. Mater.*, 2003, **15**, 4896.
- 166 J. M. Taylor, R. K. Mah, I. L. Moudrakovski, C. I. Ratcliffe, R. Vaidhyathan and G. K. H. Shimizu, *J. Am. Chem. Soc.*, 2010, **132**, 14055.
- 167 S. Kim, K. W. Dawson, B. S. Gelfand, J. M. Taylor and G. K. H. Shimizu, *J. Am. Chem. Soc.*, 2013, **135**, 963.
- 168 X. Q. Liang, F. Zhang, W. Feng, X. Q. Zou, C. J. Zhao, H. Na, C. Liu, F. X. Sun and G. S. Zhu, *Chem. Sci.*, 2013, **4**, 983.
- 169 F. Costantino, A. Donnadio and M. Casciola, *Inorg. Chem.*, 2012, **51**, 6992.
- 170 T. L. Kinnibrugh, A. A. Ayi, V. I. Bakhmutov, J. Zon and A. Clearfield, *Cryst. Growth Des.*, 2013, **13**, 2973.
- 171 S. Hudson, J. Cooney and E. Magner, *Angew. Chem. Int. Ed.*, 2008, **47**, 8582.
- 172 X. Shi, J. Liu, C. M. Li and Q. H. Yang, *Inorg. Chem.*, 2007, **46**, 7944.
- 173 X. Shi, J. P. Li, Y. Tang and Q. H. Yang, *J. Mater. Chem.*, 2010, **20**, 6495.
- 174 Y. Tang, Y. B. Ren and X. Shi, *Inorg. Chem.*, 2013, **52**, 1388.
- 175 W. T. Al-Jamal and K. Kostarelos, *Acc. Chem. Res.*, 2011, **44**, 1094.
- 176 Y. Namiki, T. Fuchigami, N. Tada, R. Kawamura, S. Matsunuma, Y. Kitamoto and M. Nakagawa, *Acc. Chem. Res.*, 2011, **44**, 1080.
- 177 C. Wang, D. M. Liu and W. B. Lin, *J. Am. Chem. Soc.*, 2013, **135**, 13222.
- 178 A. K. Gupta and M. Gupta, *Biomaterials*, 2005, **26**, 3995.
- 179 E. Duguet, S. Vasseur, S. Mornet and J.-M. Devoiselle, *Nanomedicine*, 2006, **1**, 157.
- 180 L. Lartigue, C. Innocenti, T. Kalaivani, A. Awwad, D. M. Sanchez, Y. Guari, J. Larionova, C. Guerin, J. L. G. Montero, V. Barragan-Montero, P. Arosio, A. Lascialfari, D. Gatteschi and C. Sangregorio, *J. Am. Chem. Soc.*, 2011, **133**, 10459.
- 181 H. Dong, J. Huang, R. R. Koepsel, P. Ye, A. J. Russell and K. Matyjaszewski, *Biomacromolecules*, 2011, **12**, 1305.
- 182 C. Tudisco, V. Oliveri, M. Cantarella, G. Vecchio and G. G. Condorelli, *Eur. J. Inorg. Chem.*, 2012, **32**, 5323.
- 183 H. K. Chang, F. N. Ishikawa, R. Zhang, R. Datar, R. J. Cote, M. E. Thompson and C. W. Zhou, *ACS Nano*, 2011, **5**, 9883.
- 184 K. Wang, Z. Tang, C. J. Yang, Y. Kim, X. Fang, W. Li, Y. Wu, C. D. Medley, Z. Cao, J. Li, P. Colon, H. Lin and W. Tan, *Angew. Chem. Int. Ed.*, 2009, **48**, 856.
- 185 K. E. Uhrich, S. M. Cannizzaro, R. S. Langer and K. M. Shakesheff, *Chem. Rev.*, 1999, **99**, 3181.
- 186 H. Li, T. Y. Ma, D. M. Kong and Z. Y. Yuan, *Analyst*, 2013, **4**, 1084.
- 187 E. Z. Lee, Y. S. Jun, W. H. Hong, A. Thomas and M. M. Jin, *Angew. Chem. Int. Ed.*, 2010, **49**, 9706.
- 188 M. Zhou and S. J. Dong, *Acc. Chem. Res.*, 2011, **44**, 1232.
- 189 T. Y. Ma, H. Li, Q. F. Deng, L. Liu, T. Z. Ren and Z. Y. Yuan, *Chem. Mater.*, 2012, **24**, 2253.
- 190 S. Cao, G. Gody, W. Zhao, S. Perrier, X. Y. Peng, C. Ducati, D. Y. Zhao and A. K. Cheetham, *Chem. Sci.*, 2013, **4**, 3573.
- 191 Y. P. Bi, H. Y. Hu, S. X. Ouyang, G. X. Lu, J. Y. Cao and J. H. Ye, *Chem. Commun.*, 2012, **48**, 3748.
- 192 G. Wang, B. B. Huang, X. C. Ma, Z. Y. Wang, X. Y. Qin, X. Y. Zhang, Y. Dai and M. H. Whangbo, *Angew. Chem. Int. Ed.*, 2013, **52**, 4810.
- 193 R. Cai, Y. P. Du, W. Y. Zhang, H. T. Tan, T. Zeng, X. Huang, H. F. Yang, C. P. Chen, H. Liu, J. X. Zhu, S. J. Peng, J. Chen, Y. L. Zhao, H. C. Wu, Y. Z. Huang, R. Xu, T. M. Lim, Q. C. Zhang, H. Zhang and Q. Y. Yan, *Chem. Eur. J.*, 2013, **19**, 1568.
- 194 C. S. Pan, J. Xu, Y. J. Wang, D. Li and Y. F. Zhu, *Adv. Funct. Mater.*, 2012, **22**, 1518.